Kaempferol-3-rhamnoside overaccumulation in flavonoid 3′-hydroxylase *tt7* mutants compromises seed coat outer integument differentiation and seed longevity

Regina Niñoles[1] (ID), Paloma Arjona[1], Sepideh M. Azad[1], Aseel Hashim[2], Jose Casañ[1], Eduardo Bueso[1] (ID), Ramón Serrano[1] (ID), Ana Espinosa[1], Isabel Molina[2] (ID) and Jose Gadea[1] (ID)

[1]Instituto de Biología Molecular y Celular de Plantas (IBMCP), Universitat Politècnica de València (UPV)-Consejo Superior de Investigaciones Científicas (CSIC), Ciudad Politécnica de la Innovación (CPI), Ed. 8E, C/Ingeniero Fausto Elio s/n 46022, Valencia, Spain; [2]Department of Biology, Algoma University, 1520 Queen Street East, Sault Ste. Marie, ON P6A 2G4, Canada

Summary

• Seeds slowly accumulate damage during storage, which ultimately results in germination failure. The seed coat protects the embryo from the external environment, and its composition is critical for seed longevity. Flavonols accumulate in the outer integument. The link between flavonol composition and outer integument development has not been explored.

• Genetic, molecular and ultrastructural assays on loss-of-function mutants of the flavonoid biosynthesis pathway were used to study the effect of altered flavonoid composition on seed coat development and seed longevity.

• Controlled deterioration assays indicate that loss of function of the flavonoid 3′ hydroxylase gene *TT7* dramatically affects seed longevity and seed coat development. Outer integument differentiation is compromised from 9 d after pollination in *tt7* developing seeds, resulting in a defective suberin layer and incomplete degradation of seed coat starch. These distinctive phenotypes are not shared by other mutants showing abnormal flavonoid composition. Genetic analysis indicates that overaccumulation of kaempferol-3-rhamnoside is mainly responsible for the observed phenotypes. Expression profiling suggests that multiple cellular processes are altered in the *tt7* mutant.

• Overaccumulation of kaempferol-3-rhamnoside in the seed coat compromises normal seed coat development. This observation positions *TRANSPARENT TESTA 7* and the UGT78D1 glycosyltransferase, catalysing flavonol 3-O-rhamnosylation, as essential players in the modulation of seed longevity.

Introduction

The gradual decrease in seed longevity that occurs during storage is a major concern for agriculture. The seed coat is the physical barrier between the embryo and its external environment and protects the embryo from the entry of oxygen, which progressively damages seed constituents. The Arabidopsis seed coat originates from the ovule integuments, leading to a three-layered inner integument and a two-layered outer integument in the seed, each one following a distinct path during development (Haughn & Chaudhury, 2005). Early after fertilization, cells of the innermost layer of the inner integument (the endothelium) differentiate and synthesize flavonoid polymers called proanthocyanidins (PAs). These cells also produce an endosperm-surrounding lipidic cuticle (Loubéry *et al.*, 2018). At the desiccation stage, these cells die and fuse together with the other two layers of the inner integument, constituting the brown pigment layer (BPL). The two layers of vacuolated cells of the outer integument are initially indistinguishable. About 7 days after

pollination (DAP), cells of both layers accumulate starch granules, which will degrade at later stages to reinforce cell walls. About 9 DAP, however, they diverge in fate. The external epidermal layer synthesizes mucilage (a pectinaceous carbohydrate) and secretes it to the apoplast, forcing the cytoplasm to the centre of the cell, and leaving a granule-free cytoplasmic volcano-shaped column (the columella) in the mature seed. In the inner layer of the outer integument, mainly flavonols (but not PAs) accumulate (Pourcel *et al.*, 2005). Later on, these cells synthesize suberin. Finally, both layers die and crush together, constituting the suberized palisade layer (PL; Haughn & Chaudhury, 2005).

Different compounds in the seed coat contribute to seed longevity. Lipid polyester barriers, which are specialized in sealing off specific plant tissues, are determinants for this trait. Mutants in genes required for lipid polyester biosynthesis exhibit highly permeable seed coats (Beisson *et al.*, 2007; De Giorgi *et al.*, 2015), correlating with decreased longevity (Renard *et al.*, 2020a), and accumulation of these biopolymers have the opposite effect (Renard *et al.*, 2021). The influence of flavonoids

on seed longevity is more controversial. Initially, Debeaujon *et al.* (2000) observed sensitivity to ageing in a set of mutants deficient in the flavonoid biosynthesis pathway (*transparent testa, tt*) and proposed that these compounds function as antioxidants during storage. More recently, Loubéry *et al.* (2018) demonstrated that PAs act as structural components of the endosperm-associated cuticle, and in mutants defective in PAs, this cuticle is affected or absent. This would explain their increased seed permeability, which would compromise seed longevity. Seed coat flavonols have received less attention. In particular, how they influence development of the outer integument is unknown.

Numerous reports have shown that quercetins and kaempferols, the main flavonols present in Arabidopsis seeds, modulate normal cellular physiology and may profoundly affect it when their composition is altered. *In vitro*, they inhibit phosphoinositide-kinase (Lee *et al.*, 2010; Kong *et al.*, 2011) or glucosidase (Peng *et al.*, 2016) activities and are also able to bind and affect actin function (Böhl *et al.*, 2007). If this also occurs *in planta*, the consequences would be dramatic, given the paramount function of these proteins in cell physiology. In this regard, the effect of the loss of function of phosphoinositide kinases (Ischebeck *et al.*, 2013) or the role of actin dynamics (Zhu *et al.*, 2016; Zou *et al.*, 2019) on auxin transport could be related to the well-documented function of flavonols in the inhibition of this process (Peer & Murphy, 2007).

The complex flavonol glycosylation pattern occurring *in vivo* has hampered efforts to unequivocally assign specific flavonols to particular effects. However, approaching this issue using genetic analyses is paying off in recent years. Yonekura-Sakakibara *et al.* (2014) measured flavonoid composition of different tissues of wild-type and *male sterility 1* (*ms1*) mutants and showed that, although fertile, this mutant lacks kaempferol/quercetin 3-O-β-D-glucopyranosyl-(1,2)-β-D-glucopyranosides, compromising normal pollen development. Similarly, 7-O-rhamnosylated flavonols are important for inducing the growth defects in *rol1-2*, a mutant presenting shoot growth defects (Ringli *et al.*, 2008). Finally, Yin *et al.* (2014) clearly identified kaempferol 3,7-di-O-rhamnoside as an endogenous inhibitor of polar auxin transport in shoots.

In this study, we show that loss-of-function mutations in the flavonoid 3′ hydroxylase *TRANSPARENT TESTA 7* (*TT7*) gene dramatically affect seed longevity. In *tt7* mutants, seed coat differentiation is compromised, leading to mature seeds with severe outer integument defects, such as a defective suberized PL and incomplete seed coat starch degradation. Mutants defective in seed coat starch degradation present reduced germination after ageing treatments, revealing a novel aspect contributing to this trait. These TT7-mediated defects are seed coat-specific and are not shared by other flavonoid biosynthetic mutants. Genetic analysis allowed us to trace back this defect to the overaccumulation of kaempferol-3-rhamnoside in the seed coat. Transcriptomic profiling showed altered expression of suberin genes, as well as genes involved in cell signalling and auxin-related categories in *tt7* seeds. These findings show that changes in flavonol composition can have a tremendous impact on cellular processes involved in seed coat development. Given that many abiotic stresses alter

flavonol composition, understanding the impact of these changes is of paramount importance to design high-quality seeds.

Materials and Methods

Plant material and growth conditions

All mutants used in this study are listed in Supporting Information Table S1. *tt7-7* (Appelhagen *et al.*, 2014) and *sex1-1* (Yu *et al.*, 2001) were obtained from the Nottingham Arabidopsis Stock Centre (NASC); *tt4-8, tt7-4, tt3-4, ban-1* (Routaboul *et al.*, 2006), *tt10-2* (Pourcel *et al.*, 2005), *fls1-7* (Owens *et al.*, 2008; Bowerman *et al.*, 2012) and *tt5-1* (Shirley *et al.*, 1995) were provided by Dr Isabelle Debeaujon. *sex4-3 isa 3-2, sex4-3 amy 3-2* (Kötting *et al.*, 2009) and *isa3-2 amy3-2 lda-2* (Streb *et al.*, 2012) were provided by Dr Sebastian Streb, and *ugt78d2 tt7* (Yin *et al.*, 2014) was obtained from Anthony Schäffner. *Arabidopsis thaliana* (Linnaeus) Heynhold seeds were surface-sterilized with 70% ethanol 0.1% Triton X-100 for 15 min and rinsed using sterile water. Seeds were stratified for 3 d at 4°C. Germination was carried out on plates containing Murashige and Skoog (MS) salts containing 1% (w/v) sucrose, 10 mM 2-(N-morpholino) ethanesulfonic acid and 0.9% (w/v) agar, pH 5.7. Plants were grown under glasshouse conditions (16 h : 8 h, light : dark, at 23 ± 2°C and 70 ± 5% relative humidity) in pots containing a 1 : 2, vermiculite : soil mixture. Control and mutant plants were grown simultaneously, and seeds were collected and stored under the same conditions.

Artificial ageing assays

For controlled deterioration treatment (CDT), seeds were maintained for 14 d at 37°C at 75% RH (17 d for reciprocal crosses). The elevated partial pressure of oxygen assay (EPPO) (Groot *et al.*, 2012) was performed for 5 months at 5 bar O_2 and 40% RH. Ageing treatments were performed before seed sterilization and stratification. All assays were performed on batches showing 100% germination on MS plates under nonageing conditions. For all germination assays, three replicates per genotype were performed using 30 seeds per replicate.

Biochemical assays for seed analysis

Triphenyltetrazolium salt assay was performed as in Molina *et al.* (2008). Briefly, seeds were incubated in the dark in 1% (w/v) tetrazolium red at 30°C for 8–72 h as indicated. Then, formazan was extracted and quantified as absorbance at 485 nm. For qualitative assessment of embryo viability, seed coats were gently broken and embryos were soaked in 1% tetrazolium solution for 1 d in the dark at 30°C. Images were taken with a Leica DMS1000 microscope (Leica Microsystems CMS GmbH, Wetzlar, Germany).

Mucilage staining in dry seeds was performed using 0.01% Ruthenium Red as in Western *et al.* (2001). For mucilage extrusion assay, seeds were pretreated using 0.05 M EDTA. Lipid polyester staining was performed using Sudan Red staining, as described in Beisson *et al.* (2007). For starch staining, seeds or rosettes were

boiled in 70% EtOH for 5 min. After washing using water, iodine solution was added, and after 5 min, images were taken using a camera (rosettes) or Nikon Eclipse E600 microscope (Nikon GmbH, Düsseldorf, Germany) (seeds). For DBPA (diphenylboric acid 2-aminoethyl ester) staining, seeds were incubated overnight in 0.25% DPBA containing 0.005% Triton X-100. DPBA fluorescence was monitored under a confocal microscope (AxioObserver 780; Zeiss) using a 488-nm argon laser line. Emission was monitored between 490–516 nm (kaempferol) and 535–620 nm (quercetin). Transmission electron microscopy (TEM) experiments are described in Methods S1.

Lipid polyesters and flavonoids analysis

For lipid analysis, seed samples were delipidated and dry residues were depolymerized by methanolysis in the presence of sodium methoxide. After acetylation of the CH_2Cl_2-extractable products, monomers were analysed by gas chromatography according to Methods S1. Flavonoid analysis is detailed in Methods S1.

CRISPR/Cas9 vector construction for *tt7* editing

Two sgRNAs were designed to generate *tt7* loss-of-function mutations (Methods S1). These sgRNAs were PCR-amplified with the pCBC-DT1T2 vector using primers listed in Table S2. PCR products were BsaI-digested and subcloned into the pHEE401 binary vector, containing *Zea mays* codon-optimized Cas9 under the control of an egg cell-specific promoter (Wang *et al.*, 2015). Positive constructs were introduced into *Agrobacterium tumefaciens* GV3101 and used for floral-dip transformation. Protocols for the identification of *tt7* edited plants are detailed in Methods S1.

RNA extraction and analysis

Seed total RNA extraction was performed according to Oñate-Sánchez & Vicente-Carbajosa (2008). DNA removal was performed using DNAse (E.Z.N.A). About 1 µg RNA was reverse-transcribed using the Maxima First-Strand cDNA Synthesis Kit (Thermo Fisher). qRT-PCR was performed using PyroTaq Eva-Green qPCR Mix Plus (ROX; Cultek, Madrid, Spain) in a total volume of 20 µl. Data are the mean of three replicates. Relative mRNA abundance compared with AT5G55840 (Czechowski *et al.*, 2005) was calculated using the ΔC_t method. Primers for qRT-PCR are listed in Table S2. For RNA-Seq, total RNA was extracted from developing seeds (8 DAP). Twenty million 50 nt reads per library were sequenced. Three replicates were used per genotype. Data analysis is detailed in Methods S1.

Results

The reduced longevity of *tt7* seeds is distinctive among flavonoid mutants and involves seed coat composition

Debeaujon *et al.* (2000) reported a reduced seed longevity in a set of flavonoid mutants, but the contribution to this trait of the different subgroups of flavonoids was not explored further. We assayed seed longevity in a set of mutants in the Wassilewskija (WS) and L*er* background whose flavonoid profiles are available. *tt4-8* did not contain any kind of flavonoids in their seeds, *tt5-1* contains only 7% of flavonols and no PAs, whereas *tt10-2* seeds accumulate more quercetin-derived flavonols and more soluble PAs (cyanidin-derived, the type present in wild-type Arabidopsis seeds). *ban-1* and *tt3-4* seeds did not contain PAs, whereas flavonols were absent in seeds containing mutations in the *FLAVONOL SYNTHASE* (*FLS*) gene (*fls1-7*). Finally, *FLAVONOID 3′-HYDROXYLASE* mutant seeds (*tt7-4*) did not contain quercetin-derived flavonols, but accumulate large amounts of kaempferol-derived flavonols and an unusual composition of PAs (epiafzelechin-derived; Fig. S1; Pourcel *et al.*, 2005, Routaboul *et al.*, 2006; Schulz *et al.*, 2016).

Artificial ageing assays revealed a very dissimilar response among mutants. To magnify differences, ageing conditions were adjusted so that wild-type seeds were able to germinate up to 60% in controlled deterioration treatment (CDT) and 90% in EPPO assay. Under these conditions, a complete absence of flavonoids does not dramatically affect seed longevity, as *tt4-8* seeds did not show more sensitivity than wild-type seeds, and *tt5-1* seeds showed a weak sensitivity under EPPO. Moreover, *tt10-2* seeds did not present higher longevity than the wild-type, despite containing higher amounts of flavonoids. Depleting flavonols did not affect longevity (as in *fls1-7*), and neither did the absence of PAs, as in *tt3-4*, (or only affected it partially, as in *ban-1*, whose longevity was reduced only a 25%; Fig. 1a,b). Remarkably, extreme sensitivity was observed in *tt7-4*, whose seeds present a 60% and 80% lower germination than wild-type after CDT an EPPO, respectively. This dissimilar response among mutants was also observed in Col-0 background, including the dramatic reduction in longevity observed in the *tt7-7* allele, which contains a pattern of seed flavonoid composition similar to *tt7-4* (Fig. S1).

Proanthocyanidins are accumulated in the seed coat, but flavonols are present both in maternal (seed coat) and in zygotic (embryo and endosperm) tissues (Fig. S2a–c; Routaboul *et al.*, 2006). To discern which of these two structures is involved in the seed longevity defect of *tt7* mutants, we conducted reciprocal crosses using the *tt7-7* allele. F1 seeds of wild-type plants that were pollinated with *tt7* pollen showed a response similar to the wild-type after the ageing treatment. By contrast, F1 seeds of *tt7* plants pollinated with wild-type pollen retained the reduction in seed longevity after CDT observed for *tt7* (Fig. 1c). These results, together with the fact that *tt7* fresh seeds germinate perfectly (Fig. S3a), and that *tt7* embryos presents normal morphology (Grunewald *et al.*, 2013, Fig. S3b–e), suggest that the seed coat is responsible for the reduced seed longevity observed in *tt7* mutants after CDT.

Tetrazolium uptake is a proven method for analysing seed permeability in Arabidopsis seeds (Molina *et al.*, 2008). Quantitative assays after a 72 h incubation revealed that the different *tt* mutants present different degrees of permeability to tetrazolium (Fig. 1d). Control experiments ruled out the possibility that differences in signal results from defects in viability or from the ability to reduce tetrazolium salts (Fig. S4a,b). We observed that *tt3-4*, *tt4-8*, *tt7-4*, *ban-1* and *fls1-7* seeds were more permeable to tetrazolium salts. In particular, a 1.8-fold increase in absorbance
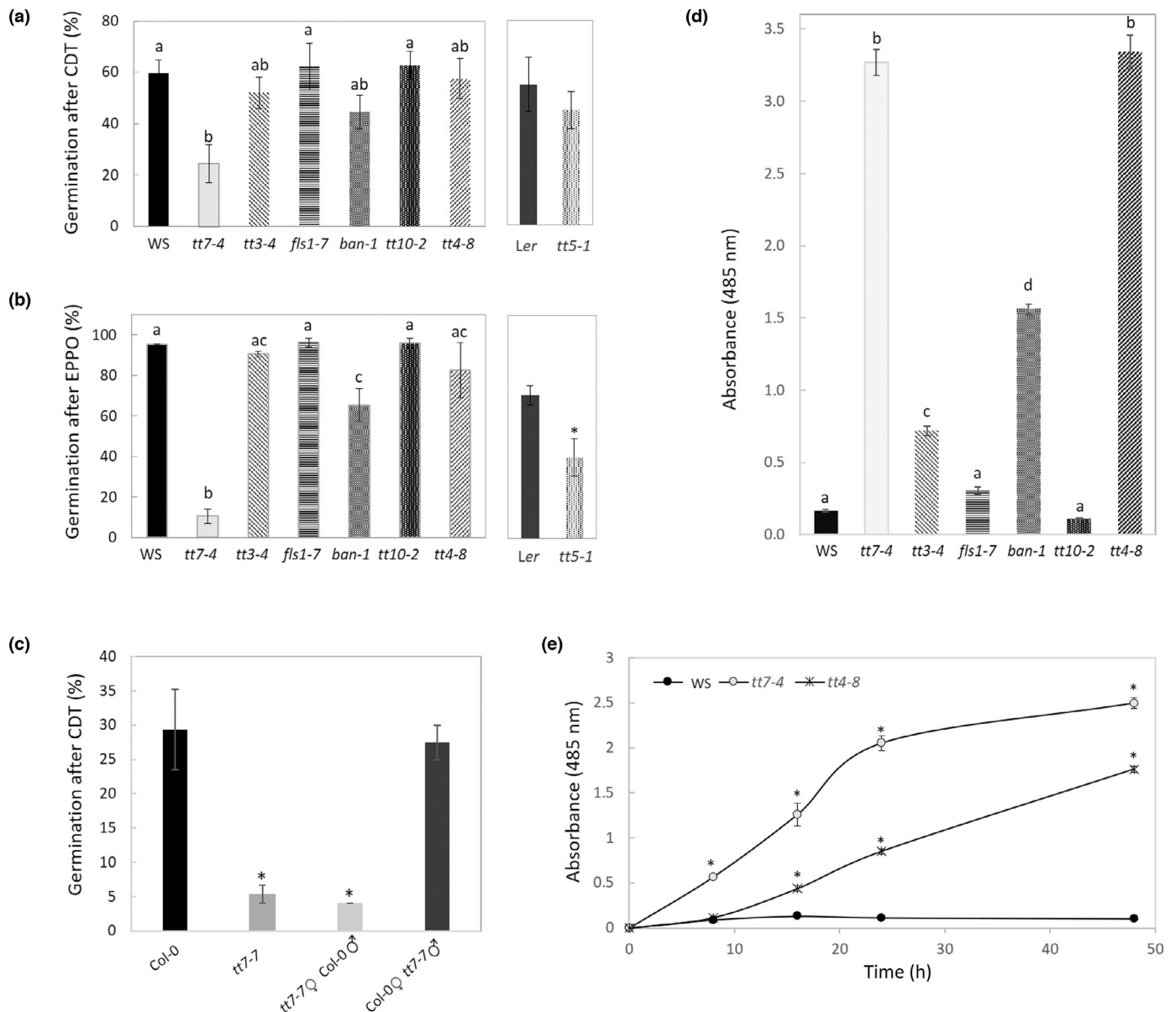
Fig. 1 Seed longevity and permeability of different *transparent testa* mutants. Seed longevity in *tt7* reciprocal crosses. Seeds were incubated for 14 d at 75% RH (controlled deterioration treatment (CDT) (a), or 5 months at 5 bar O_2 and 40% RH (elevated partial pressure of oxygen assay, EPPO) (b). Germination was recorded after 5 d. One-way ANOVA and Tukey *post hoc* analysis was used to compare different genotypes. Letters represent significant differences at $P < 0.05$. (c) Seeds from wild-type (Col-0), *tt7-7* and F1 from reciprocal crosses were subjected to CDT, and germination was recorded after 5 d. Bars represent the average and SE of three replicates. WS, Wassilewskija; Ler, Landsberg *erecta*; Col-0, Columbia-0. (d) Wild-type (WS) and mutant seeds were incubated for up to 48 h (e) and 3 d in 1% tetrazolium at 30°C. Formazan was quantified by absorbance at 485 nm. Data are the mean and SE of three biological replicates. Asterisks indicate significant differences with WT ($P < 0.05$) in a two-tailed Student *t*-test.

was observed for *fls1-7*, 4.5-fold for *tt3-4* and 9.7-fold for *ban-1* seeds, compared with wild-type. Intriguingly, *tt7-4* and *tt4-8* were by far the most permeable mutants, with increases of > 20-fold. When the assay was performed at shorter incubation times, *tt7-4* showed a higher signal than *tt4-8*, (Fig. 1e), suggesting a faster entry of tetrazolium into the seeds. For most of the mutants, there is an inverse correlation between permeability and longevity, with *tt7-4* observed to be the most sensitive to ageing and the one with the most permeable seed coat. For *tt4-8*, by contrast, seeds were not sensitive to CDT despite having highly permeable seed coats, possibly indicating the existence of a

compensatory effect in this mutant. Taken together, these results indicate that, among all mutants tested, *tt7* is the most sensitive to seed ageing. This sensitivity has a maternal origin and *tt7* seeds were the most permeable among those analysed here, suggesting a severe and distinctive defect in the seed coat of this mutant.

The outer integument is defective in *tt7* mutants

Mucilage and lipid polyesters contribute to the physiological properties of the seed coat. We initially investigated the ability of flavonoid mutants to properly develop these two structures using

biochemical assays. When Arabidopsis wild-type seeds were hydrated, the seed coat mucilage swelled rapidly, and a pink-stained capsule was observed after ruthenium red staining. By contrast, in *tt7-4*, the mucilage was severely affected, being

drastically reduced or absent in >75% of the *tt7* seeds (Figs 2a, S5a). EDTA treatment of *tt7* seeds did not increase the percentage of seeds releasing the trapped mucilage, suggesting that *tt7* is defective in mucilage biosynthesis and not in extrusion
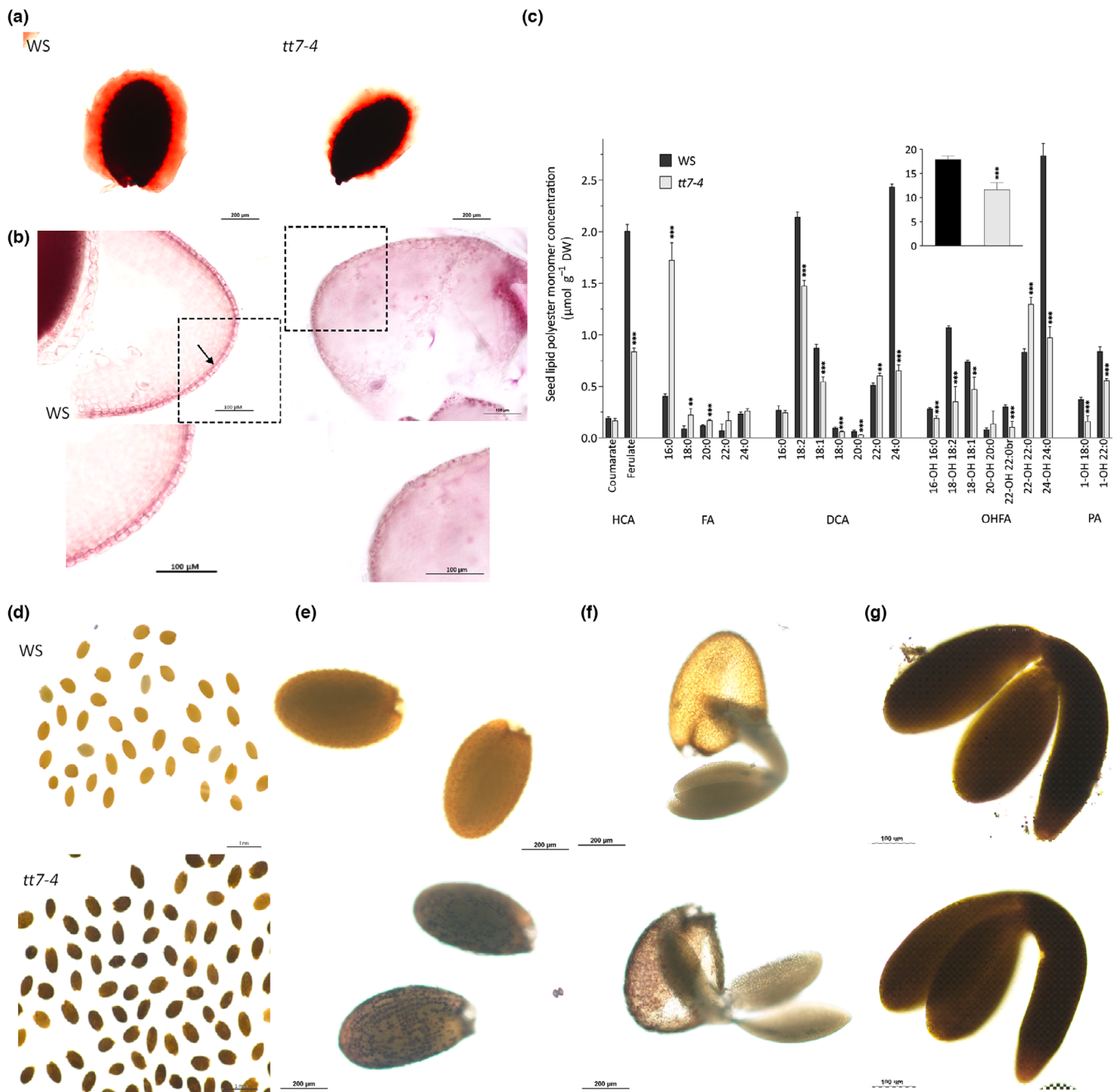

Fig. 2 Seed coat development is affected in *tt7*. (a) Representative images of Wassilevskija (WS) and *tt7-4* seeds after staining with ruthenium red for 15 min. Bars, 200 μm. (b) Representative images of WS and *tt7-4* seeds stained with Sudan Red. Black boxes show zoomed areas in lower panels. Arrows indicate lipid polyester region in the subepidermal layer. Bar, 100 μm. (c) Lipid polyester monomer composition of WS and *tt7-4* mutant seeds. Bars represent the mean content of each identified monomer and error bars represent SD. Asterisks indicate significant differences with WT: *, $P < 0.05$; **, $P < 0.01$; ***, $P < 0.001$; two-tailed Student *t*-test. br, branched monomer; DCA, dicarboxylic acids; FA, fatty acids; HCA, hydroxycinnamic acids; OHFA, hydroxyfatty acids; PA, primary fatty alcohols; WS, Wassilevskija. Inset: Total amount of lipid polyester monomers released after depolymerization of WS and *tt7-4* seeds. (d) Image of WS and *tt7-4* dry seeds after iodine staining. Bar, 1 mm. (e) Amplified view of WS and *tt7-4* dry seeds after iodine staining. Bar, 200 μm. (f) Representative images of WS and *tt7-4* seed coat and embryo from dry seeds stained with iodine. Only the *tt7-4* seed coat is stained. Bar, 200 μm. (g) Representative images of WS and *tt7-4* developing embryos (12 d after pollination, DAP) stained with iodine. Bar, 100 μm.

(Fig. S5b). After staining seeds with Sudan Red to visualize seed coat lipid polyesters, wild-type seeds showed the characteristic pink layer in the outer integument of the seed coat. This layer was not visible in *tt7-4*, suggesting that lipid polyester deposition is compromised (Fig. 2b). Chemical analysis of lipid polyester composition in dry seeds revealed an overall *c.* 30% reduction in the amounts of monomers released after depolymerization in the *tt7-4* mutant, as compared to wild-type (Fig. 2c inset). Most lipid monomers were significantly reduced in *tt7-4*, with the exception of three 22 : 0 straight chain suberin components (Fig. 2c) and fatty acids with up to 22 carbons, which showed higher accumulation in the mutant. Similar results were observed in the *tt7-7* allele (Fig. S6).

These findings were confirmed by TEM (Figs 3a,b, S7). In wild-type dry seeds, the columella is clearly observed in the external layer of the outer integument. Beneath the epidermis lies the dark suberin-containing PL. In *tt7*, columella-like structures were identified, indicating that the outer cells secreted some mucilage that forced the protoplast towards the centre of the cell. However, this structure is only insinuated, being reminiscent of the initial stage of columella formation at the torpedo stage in wild-type seeds, except for the characteristic starch granules at the centre of the epidermal cells in this stage (Windsor *et al.*, 2000). In the inner layer of the outer integument, the defined electron-dense layer of suberin is not properly formed. Starch granules, present in wild-type seed coats only at earlier stages, are highly abundant
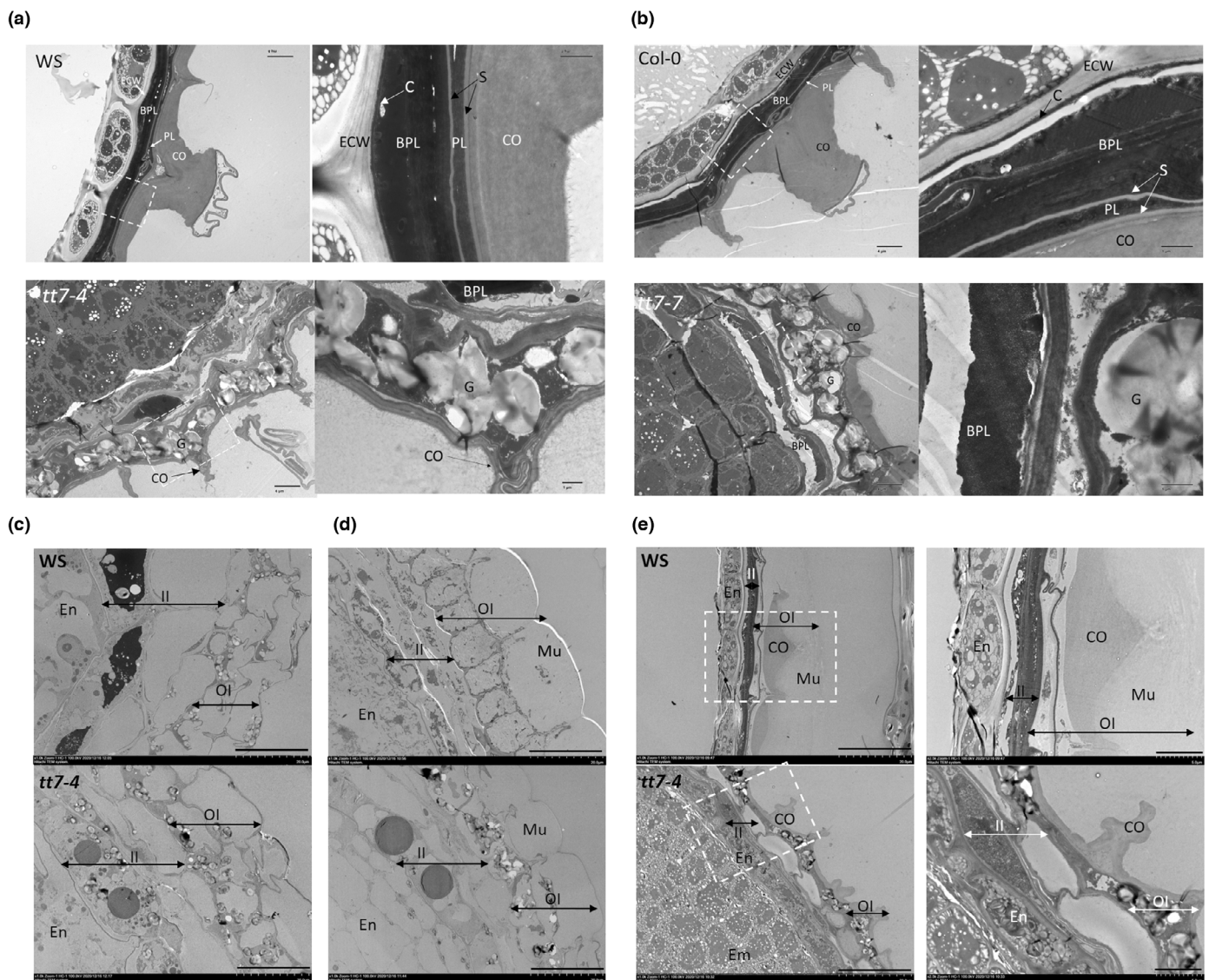

Fig. 3 Ultrastructural analysis of wild-type and *tt7* seed coats. Representative transmission electron microscopy (TEM) images of Wassilevskija (WS) and *tt7-4* (a) and Col-0 and *tt7-7* (b) dry seeds. White boxes indicate zoomed areas in the right panels. Bars: (left panels) 4 μm; (right panels) 1 μm. Representative TEM images of seed coats of WS (above) and *tt7-4* mutant (below) at 7 d (c), 9 d (d) and 16 d (e) after pollination. White boxes in (e) indicate zoomed areas in the right panels. Bars: (c, d, e left panels) 20 μm; (e right panel) 5 μm; BPL, brown pigment layer; C, cuticle; CO, columella; Col-0, Columbia 0; ECW, endosperm cell wall; En, endosperm; G, granules; II, inner integument; Mu, mucilage; OI, outer integument; PL, palisade layer; S, suberin. Lipid polyesters (C, S) are not appreciated in *tt7* preparations.

and distributed along the cells, as previously observed by Lu *et al.* (2008). The defects in *tt7* outer integument start to be visible at 9 DAP, when the developmental fate of the two layers diverge. At 3 DAP, the five integumental layers are well-formed in *tt7* seed coats (Fig. S8). At 7 DAP, the highly vacuolated large cells of the two external layers are observed in wild-type, together with the endothelium beneath them, with the electron-dense tannin vacuole covering the whole cytoplasm. This same structure is present in *tt7*, with the appearance of large round dense globules in the cytoplasm of endothelial cells being the only distinct feature (Fig. 3c). Similar to wild-type, the *tt7* epidermis does not contain granules and produces mucilage at 9 DAP, with cytoplasm forced to generate pin-like structures perpendicular to the seed surface. In the inner layer, however, starch granules continue to accumulate, pushing the vacuole towards the inner region of the cell (Fig. 3d). Cell walls are not reinforced, explaining the less-defined structure of this layer (Fig. S9). At 16 DAP, *tt7* columella is clearly defective, and inner cells still contain granules, that remain present until maturity (Fig. 3e).

Starch accumulation in *tt7* seed was seed coat-specific (Figs 2d–f, S10), as embryo (Fig. 2f,g; Andriotis *et al.*, 2010) and leaf starch (Fig. S11) was properly synthetized and degraded. Taken together, these results indicate that differentiation of the outer integument (specifically lipid polyesters biosynthesis and starch metabolism) is altered in *tt7* mutants.

Accumulation of a kaempferol derivative is responsible for the seed coat and longevity defects of *tt7*

We next investigated whether the defects observed in *tt7* seed coats were shared by other flavonoid mutants. Similar to wild-type, *tt3-4*, *tt4-8*, *tt10-2* and *fls1-7* seeds were able to produce mucilage. In *ban-1* and *tt5-1*, the amount of mucilage was reduced. A lipid polyester layer was also visible in all mutants using Sudan Red staining (Fig. 4a), supporting data published in Col-0 for *tt3*, *ban* and *tt10* (de Silva *et al.*, 2021). Seed coat starch accumulation at maturity was not observed in any of the mutants (Fig. S12). These findings were confirmed by TEM observation of *tt4-8*, *fl1-3* and *ban-1* seed coat sections at maturity (Fig. 4b). In these mutants, the ultrastructure of the outer integument was similar to that of wild-type seeds. Therefore, the specific altered flavonoid pattern of *tt7* seems to cause its distinctive phenotypes. A flavonoid-deficient *tt7-4 tt4-8* double mutant was generated to confirm this hypothesis, but the defects observed in lipid polyesters and starch accumulation in *tt7* mutants were not observed in *tt7-4 tt4-8* seeds (Fig. 5a,b). Similarly, the sensitivity to ageing of *tt7-4* seeds was abolished in *tt7-4 tt4-8*, indicating that *tt7* defects are flavonoid-dependent, and not due to nonflavonoid-related activities of the TT7 protein (Fig. 5c).

Two features are characteristic of the *tt7* flavonoid profile: a dramatic increase in kaempferol-derived flavonols and an altered composition of PAs (Routaboul *et al.*, 2006). To discern which of these two groups of flavonoids is responsible for the *tt7* phenotype, *TT7* was chosen as target to generate CRISPR-edited plants in *tt3-4* or *fls1-7* mutant backgrounds. A *tt3 tt7* double mutant is expected to accumulate kaempferols, but not PAs, whereas *fls1*

tt7 is not expected to accumulate kaempferols but would contain PAs. To generate these lines, we used the promoter of the egg cell-specific EC1.2 gene to drive the expression of Cas9, and two guide RNAs to create an internal deletion in the *tt7* gene, leading to homozygous knock-out mutants (Wang *et al.*, 2015; Methods S1; Fig. S13). Seeds from T1 *fls1-7* or *tt3-4* plants, homozygous for CRISPR-edited *tt7* (cr), were assayed for seed coat components (lipids and starch) and analysed to assess their longevity. As shown in Figs 5(a,b), S14(a), *fls1-7 tt7cr* seeds (L38 and L47) lost the *tt7* phenotypes and recover wild-type appearance. In addition, they lost the sensitivity to ageing observed in *tt7* (Fig. 5d). Conversely, *tt3-4 tt7cr* seeds (L20 and L8) retain the structural *tt7* defects in the outer integument (Figs 5a,b, S14b). Moreover, they retain the reduced seed germination after CDT, characteristic of *tt7* (Fig. 5e). As expected, *tt3-4 tt7cr* seeds were depleted in PAs, isorhamnetins and quercetins, but exhibit overaccumulation of kaempferol compounds, in a pattern similar to that reported by Routaboul *et al.* (2006) and Kerhoas *et al.* (2006) for *tt7* (Fig. S15). Five major kaempferol derivatives were found to accumulate in the *tt3-4 tt7cr* mutant: kaempferol-3-rhamnoside (K-3-R) and kaempferol 3,7-di-rhamnoside (K-3,7-di-R) at high levels, kaempferol 3-Glucoside-7-Rhamnoside (K-3-G-7-R) and kaempferol-3-rhamnoside-7-glucoside (K-3-R-7-G) at moderate levels, and kaempferol 3-glucoside (K-3-G) at lower levels, as well as kaempferol aglycone (Fig. 6a). Taken together, these results suggest that the defects observed in *tt7* seed coat are due to excess accumulation of at least one of these kaempferol derivatives in this structure.

The *tt7* seed coat phenotype is correlated with kaempferol 3-O-rhamnoside overaccumulation

To identify the kaempferol compound/s responsible for the *tt7* phenotype in seed coat development and longevity, we blocked kaempferol glycosylation at specific steps. To achieve this, we used double mutants in *tt7* and in the major UDP-dependent flavonol glycosyltransferases (UGTs) responsible for the conjugation of the most abundant flavonol compounds in leaves. UGT78D1 and UGT78D2 catalyse the transfer of rhamnose and glucose to the 3-OH position of flavonols, respectively. The major form of 7-O-conjugation is 7-O-rhamnosylation, catalysed by UGT89C1. UGT73C6 contributes to 7-O-glucosylation, although only trace amounts of flavonols are 7-O-glucosylated (Jones *et al.*, 2003; Yonekura-Sakakibara *et al.*, 2007). Whereas a *tt7 ugt78d2* line was available (Yin *et al.*, 2014), CRISPR-edited (cr) *tt7* lines were generated in *ugt78d1* and *ugt89c1* mutant backgrounds (Yin *et al.*, 2014; Methods S1; Fig. S16). Accordingly, *tt7 ugtd2* seeds, unable to glucosylate in 3-OH, would not accumulate K-3-G and K-3-G-7-R. This line retained the *tt7* phenotype, showing strong starch accumulation in the seed coat and decreased seed longevity (Fig. 6b,c). The *ugt78d1 tt7cr* seeds were unable to accumulate 3-O-rhamnosylated kaempferols (K-3-R, K-3,7-di-R and K-3-R-7-G), but maintained the ability to synthesize K-3-G-7-R. The *ugt89c1 tt7cr* line, by contrast, was unable to accumulate K-3,7-di-R, but still accumulates high amounts of K-3-R and K-3-R-7-G, this last compound likely produced by UGT73C6 (Jones
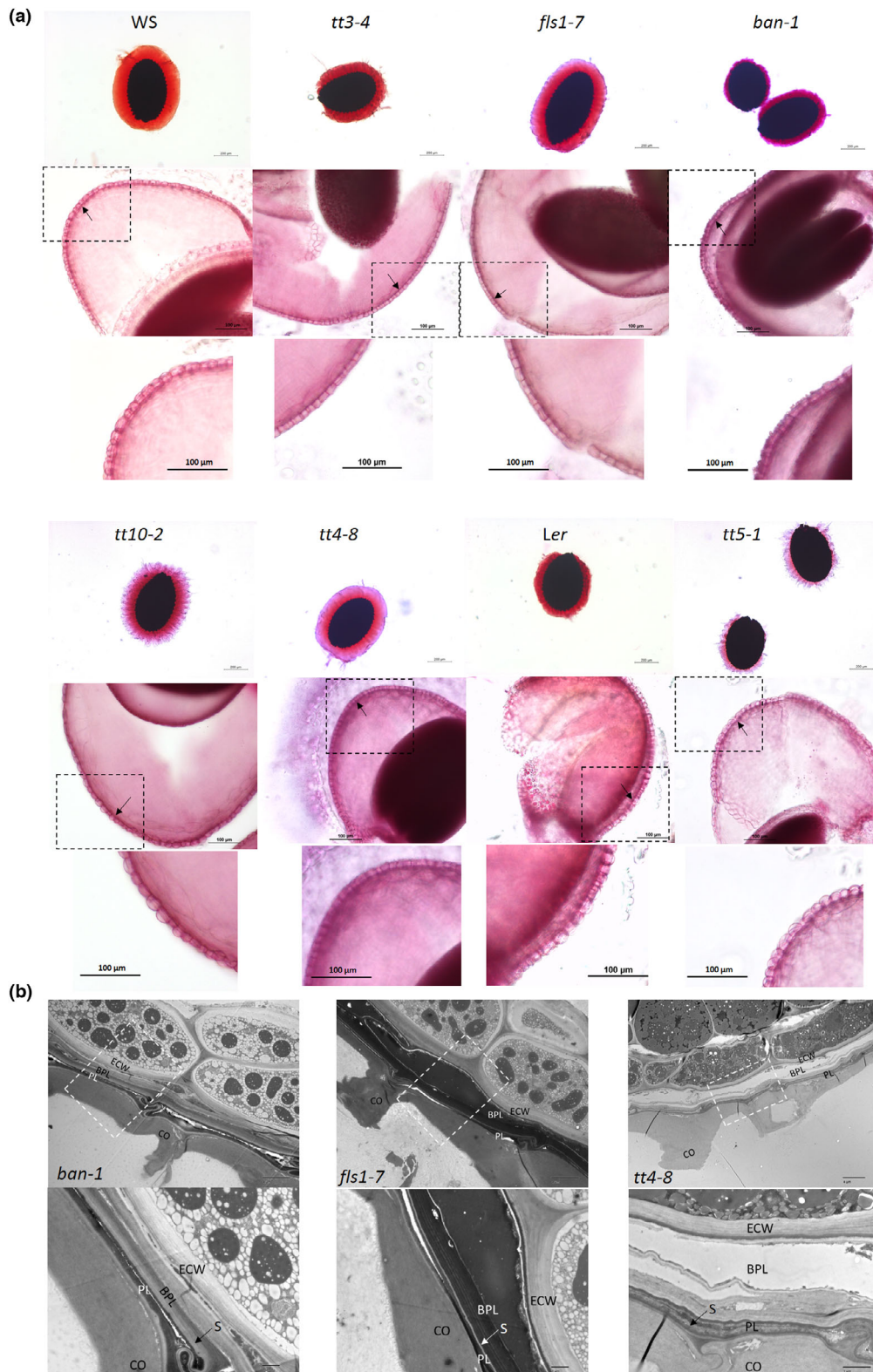
Fig. 4 Comparative analysis of *transparent testa* seed coats. (a) Ruthenium red (above) and Sudan Red (below) staining of different *tt* mutants showing mucilage and polyester layers. Bars: (top panels) 200; (middle and bottom panels) 100 μm, respectively. Black boxes show zoomed areas in lower panels. Arrows indicate lipid polyester layer. (b) Representative transmission electron microscopy images *ban1*, *fls1-7* and *tt4-8* seed coats. White boxes indicate zoomed areas in panels below. Bars: (top panels) 4 μm; (bottom panels) 1 μm; BPL, brown pigment layer; CO, columella; ECW, endosperm cell wall; PL, palisade layer; WS, Wassilevskija.
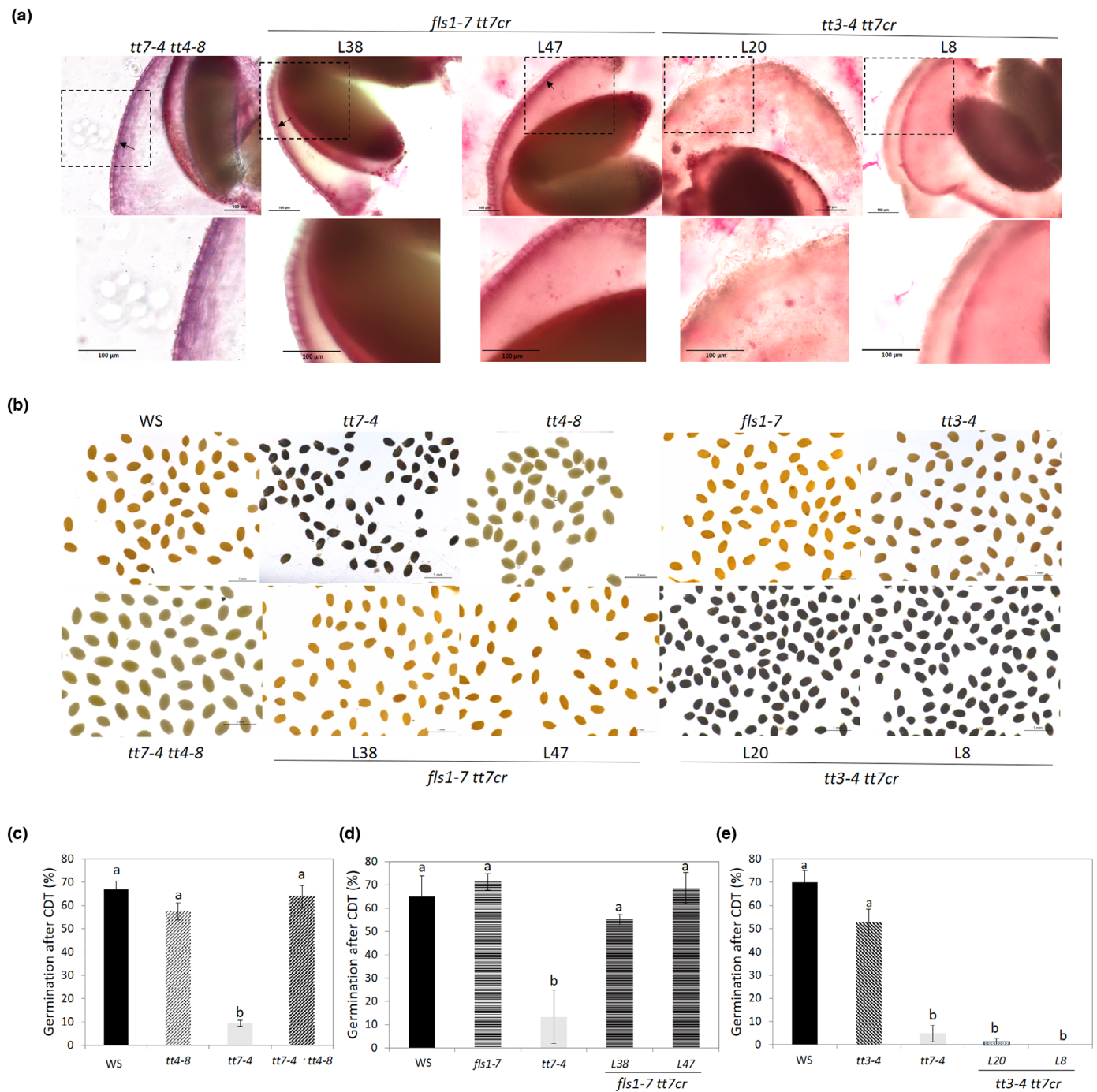
Fig. 5 Seed coat defects in *tt7* correlate with overaccumulation of a kaempferol derivative. Representative image of *tt7-4 tt4-8* and two lines obtained by edition of the *TT7* gene in a *fls1-7* (L38 and L47) and *tt3-4* (L20 and L8) mutant backgrounds. (a) Sudan Red staining; bar, 100 μm. Arrows indicate lipid polyester layer. Black boxes show zoomed areas in lower panels. (b) Iodine staining. Bar, 1 mm. (c–e) Percentage of germination after controlled deterioration treatment (CDT). Seeds were incubated for 14 d at 75% RH. Germination was recorded after 5 d. Bars represent the average and SE of three replicates using 30 seeds per genotype. A one-way ANOVA and Tukey *post hoc* analysis was used to compare different genotypes. Letters represent significant differences at $P < 0.05$. WS, Wassilewskija.

et al., 2003; Fig. 7). Levels of kaempferol aglycone were similar in the three mutants. Neither starch accumulation in the mature seed coat, nor suberin and seed longevity defects were observed in *ugt78d1 tt7cr* seeds, indicating that the lack of *UGT78D1* supresses the *tt7* phenotypes (Figs 6b,c, S17). This suppression was not observed in *ugt89c1 tt7cr* seeds, clearly pointing to K-3-R or K-3-

R-7-G as the two compounds putatively responsible for the seed coat defects in *tt7*. *UGT73C6*, responsible for flavonol 7-O-glucosylations, is expressed in seeds at very low levels (Belmonte *et al.*, 2013; Waese *et al.*, 2017). RT-qPCR experiments indicate that, within the seed, this gene is hardly expressed in the seed coat and mainly expressed in the embryo, confirming previous data
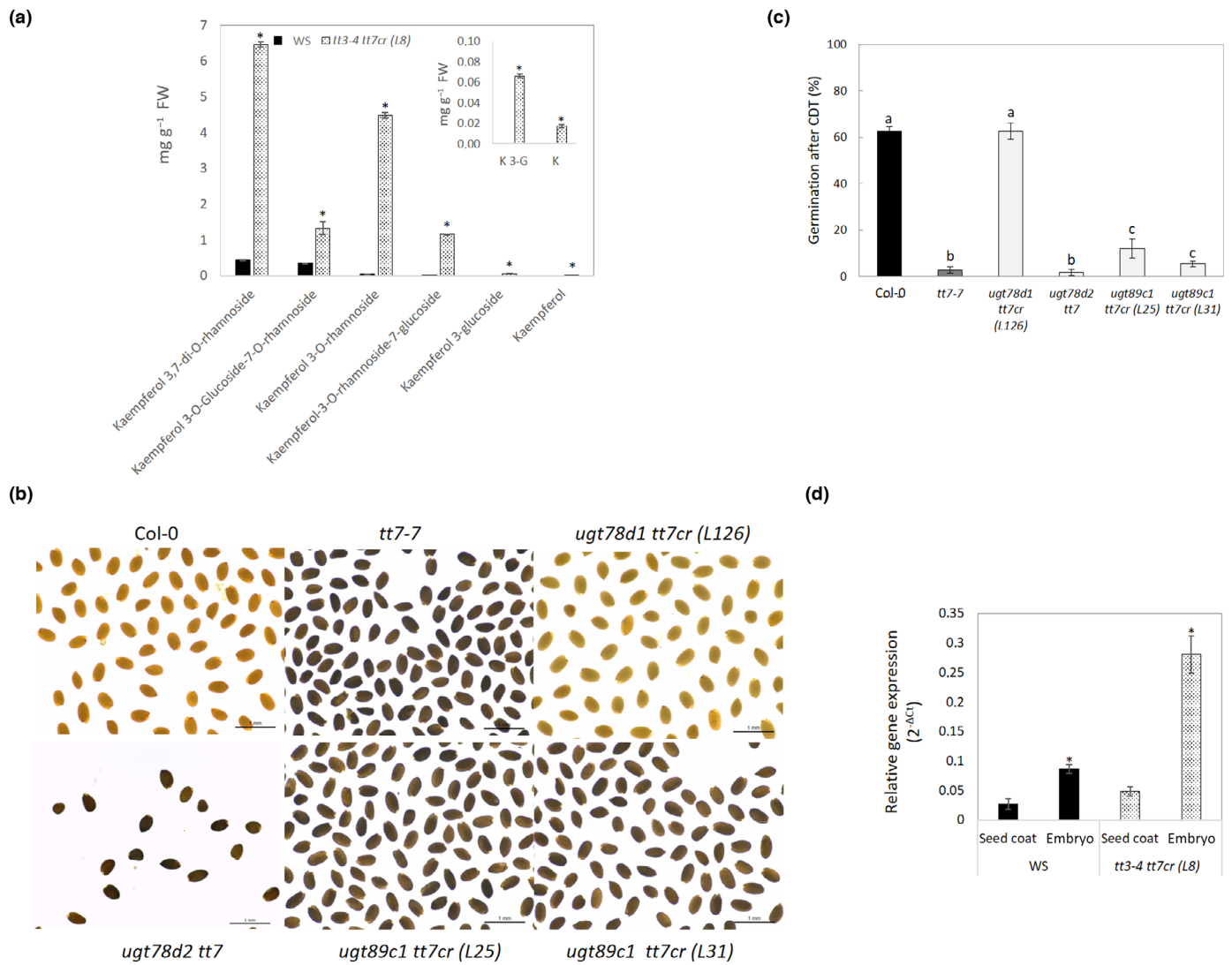
Fig. 6 *tt7* phenotype correlates with overaccumulation of kaempferol 3-rhamnoside (a) Kaempferol derivatives content of *tt3tt7cr* (L8) seeds measured using liquid chromatography–mass spectrometry analysis. The means and SE of three biological replicates are shown. Flavonols were quantified using kaempferol aglycone as a standard. Asterisks indicate significant differences with WT ($P < 0.05$) in a two-tailed Student t-test. K-3-G, Kaempferol 3-Glucoside; K, Kaempferol. (b) Iodine staining of *ugtd1 tt7cr*, *ugtd2 tt7* and *ugtc1 tt7cr* mutants. (c) Percentage of germination after CDT. Seeds were incubated for 14 d at 75%. Germination was recorded after 5 d. Bars represent the average and SE of three replicates. Letters represent significant differences at $P < 0.05$ after a one-way ANOVA and Tukey *post hoc* analysis ($P < 0.05$). (d) Expression levels of *UGT73C6* gene were determined by real-time quantitative PCR in seed coat and embryo of WS and *tt3-4 tt7cr* developing seeds (10–14 DAP). Relative expression compared with the endogenous gene AT5G55840 is shown. Data are the mean of three replicates. Asterisks represent significantly differing from the wild-type in a two-tailed Student t-test ($P < 0.05$). Bars represent the average and SE of three replicates. WS, Wassilewskija.

(Belmonte *et al.*, 2013; Fig. S18). Interestingly, in a *tt7* background, this difference in expression between seed coat and embryo was increased (Fig. 6d). Given this pattern of expression, we assume that K-3-R-7-G is accumulated mainly in the embryo and not in the seed coat. Accordingly, we conclude that the best candidate to be responsible for the seed coat phenotypes in *tt7* backgrounds is kaempferol-3-rhamnoside.

Starch degradation in the seed coat is needed for seed longevity

We recently demonstrated the role of suberin in the regulation of seed longevity (Renard *et al.*, 2020a, 2021). Accordingly, the

sensitivity to ageing of *tt7* seeds can be partially explained by its defective suberin layer. To determine whether starch accumulation could also be influencing seed longevity, a genetic approach using mutants accumulating starch in the seed coat was employed. Moderate starch accumulation in mature seeds of *sex1* and *sex4* has been described (Andriotis *et al.*, 2010). In leaves, the most severe starch phenotype appears in the triple mutant *amy3 isa3 lda*, which completely prevents starch breakdown (Streb *et al.*, 2012). Despite the wild-type pattern of seed starch accumulation in the single mutants (Andriotis *et al.*, 2010), this triple mutant strongly accumulates starch in dry seeds, especially in the seed coat (Fig. S19a,c). Longevity effects were not observed for *sex1-1*, *sex4-3 isa3-2* and *sex4-3 amy3-2* after CDT assays, suggesting that the defects of *sex1* or *sex-4*
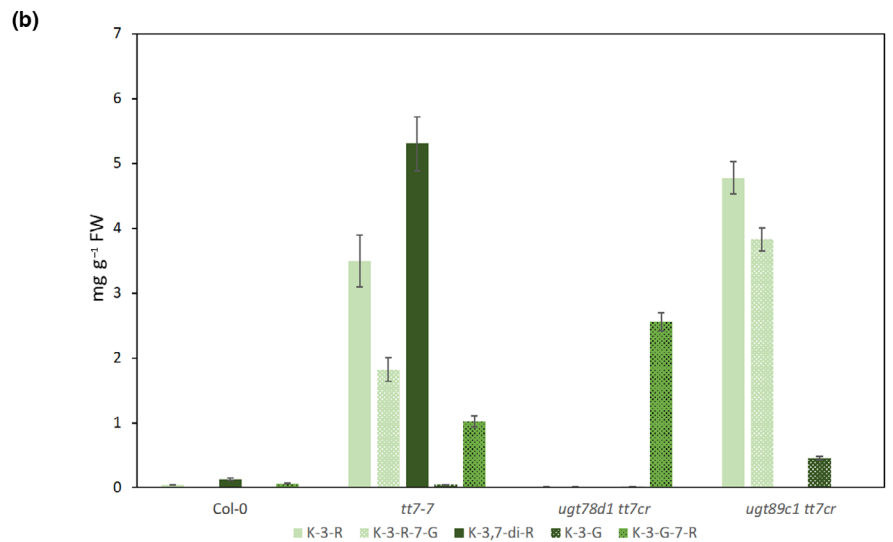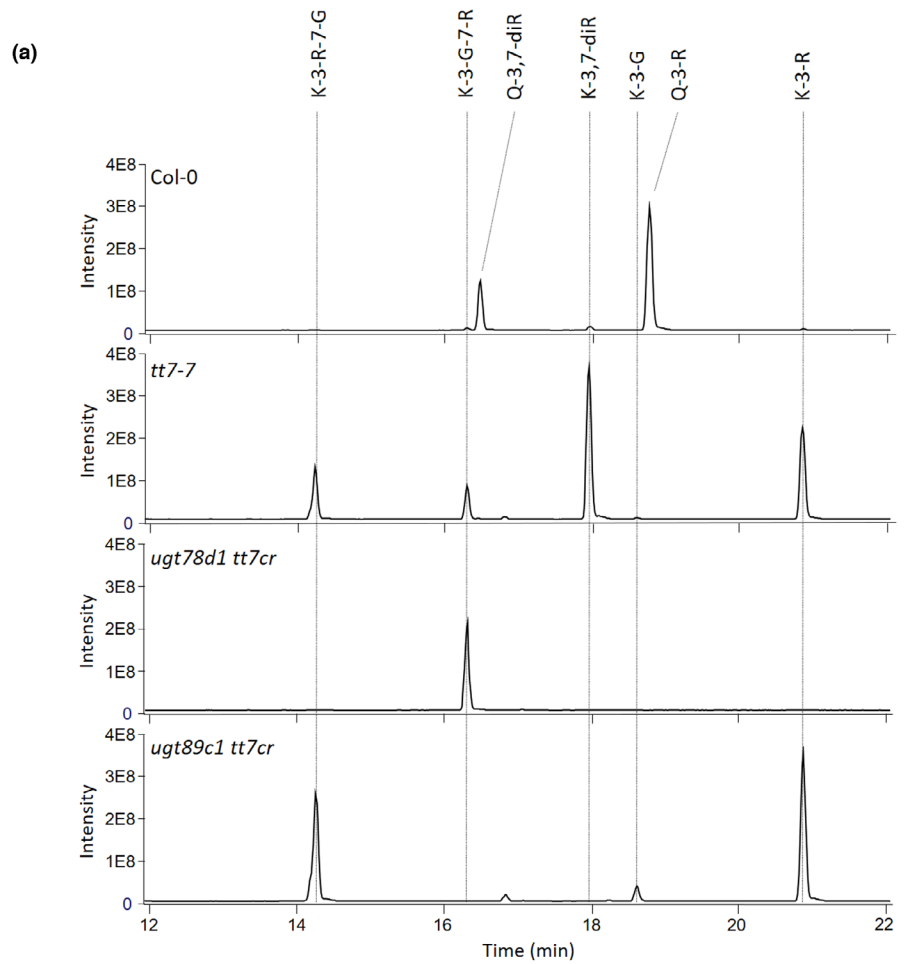
Fig. 7 Flavonol glycoside pattern in Col-0 and *tt7-7*, *ugt78d1 tt7cr* and *ugt89c1 tt7cr* mutants obtained by UPLC-MS analysis. (a) Comparative analysis of seed kaempferol glycosides in the different mutants. Major quercetin glycosides in Col-0 are marked. The same scale is used for comparison. (b) Quantification of kaempferol glycosides in the indicated genotypes. Results are means of three biological replicates. Error bars represent SD. Kaempferol glycosides were quantified using kaempferol aglycone as a standard.

are not sufficient to compromise longevity. Interestingly, *amy3 isa3 lda* was very sensitive to ageing, with only 38.8% germination vs 72.7% in wild-type, suggesting that when starch breakdown is severely blocked in the seed coat, longevity is affected (Fig. 8). This

mutant does not present a dramatic increase in seed permeability (Fig. S17), suggesting that seed coat starch is not used as a reserve for lipid biosynthesis, and representing a novel component involved in seed longevity independent of this property.
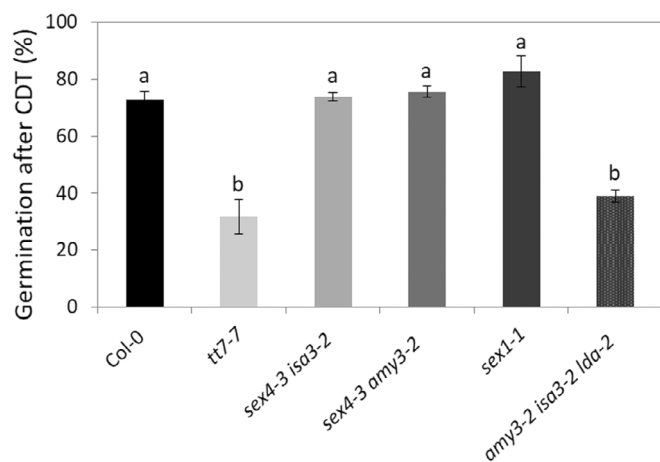
Fig. 8 Seed longevity in seed coat starch accumulation mutants. Percentage of germination of Col-0, *tt7-7*, *sex4-3 isa3-2*, *sex4-3 amy3-2*, *sex1-1* and *amy3-2 isa3-2 lda-2* mutant seeds after controlled deterioration treatment (CDT). Seeds were incubated for 14 d at 75% RH. Germination was recorded after 5 d. Bars represent the average and SE of three replicates. Col-0, Columbia 0. A one-way ANOVA and Tukey *post hoc* analysis was used to compare different genotypes. Letters represent significant differences at $P < 0.05$.

Global expression analysis reveals that cell trafficking and cell communication processes are altered in *tt7* seeds

To provide more clues about possible pathways affected by TT7 activity, transcriptome profiling was performed at 8 DAP, 1 d after the peak of *TT7* expression during seed development (Winter *et al.*, 2007; Belmonte *et al.*, 2013) in Col-0 and *tt7-7* seeds. A total of 4289 genes showed significant differentially expressed genes (DEGs) in *tt7* compared with wild-type (Table S3). First, we reanalysed the data published by Hildreth *et al.* (2022) for *tt4* in seedlings and intersected them with our *tt7* DEGs, using the same filtering criteria. Five times more genes were found DE in *tt7*, and only 4.2% of them (184 genes) were common to both datasets (Fig. S20). This suggests that our analysis of the *tt7* transcriptome can be useful to provide clues that explain *tt7*-specific phenotypes, further than those consequence of the lack of quercetin-derived flavonols. Pruned Gene Ontology (GO) term analysis among DEGs in the mutant showed enrichment of 313 functional categories in the Biological Process, and 118 in the Molecular Function GO classification, indicating that disruption of TT7 activity provokes a dramatic readjustment of cell biology. Among the categories enriched in the 2284 *tt7* upregulated genes (Table S3; the top 20 nonredundant terms are shown in Fig. 9a,b), it is remarkable the appearance of cytoskeleton-related categories, such as actin filament-based movement (GO:0030048), which includes the concerted upregulation of myosins, and phosphatidylinositol-related processes (GO:0046488, GO:0052866 and GO:0016307), including the upregulation of phosphatidylinositol-kinases and phosphatases. Moreover, cell communication-related categories, such as signalling (GO:0023052), movement of cell or subcellular component (GO:0006928) and cell communication (GO:0007154) including the coordinated upregulation of kinesins, as well as some calcium sensors and kinases, were also enriched. Finally, the category

(1→3)-β-D-glucan biosynthetic process (GO:0006075) was overrepresented by the concerted upregulation of eight isoforms of callose synthase genes, involved in plasmodesmata regulation. Detailed differential expression data of genes belonging to these categories are shown in Table S4. Among the 2005 DEGs downregulated in *tt7*, there was a remarkable enrichment in plant-type cell wall organization or biogenesis (GO:0071669), including the downregulation of cell wall enzymes, such as expansins and cellulose synthases, as well as in the lipid localization term (GO:0010876), including the downregulation of lipid transfer proteins, and lipid metabolism (GO:0006629), with the downregulation of diverse lipid metabolism enzymes (Fig. 9c,d). Thus, global transcriptomic results suggest that *tt7* mutants have defects in cellular components such as the cytoskeleton or plasmodesmata, as well as disfunction of molecular switches involved in cell signalling, organelle trafficking and lipid biology.

Discussion

Despite being one of the best-studied secondary metabolite pathways in plants, the function of flavonoids in the seed coat is not completely understood. Although flavonoid biosynthesis has been considered important for seed longevity since Debeaujon *et al.* (2000) showed that a set of mutants (*transparent testa*, *tt*) presented increased seed deterioration upon ageing, the molecular link between the defects in these mutants and seed longevity is still uncertain, as well as how essential flavonoids are for this trait. Their antioxidant properties were invoked to explain this effect, although the contribution of flavonoids to the integrated antioxidant system of plants is under debate (Hernández *et al.*, 2009).

Arabidopsis seeds accumulate flavonols and PAs (Lepiniec *et al.*, 2006). Given their seed coat specificity and that the *tt* phenotype refers to the lack of brown colour provided by these compounds, PAs received more attention than seed coat flavonols as candidates to be the main flavonoids involved in seed protection. Although some contribution to restrain oxidative damage during storage cannot be discarded, this does not explain why mutant seeds completely deployed of PAs but maintaining their content of flavonols (*tt3-4*), or with increases in PA amounts (*fls1-7*, *tt10-2*) present similar rates of deterioration than wild-type seeds after EPPO treatment, which mimic oxidative conditions (Groot *et al.*, 2012). Even the complete absence of flavonoids (including PAs, *tt4-8*) does not dramatically impact seed longevity, as previously reported (Debeaujon *et al.*, 2000; Clerkx *et al.*, 2004), suggesting that the intrinsic presence of PAs (or flavonols) in the seed coat, and hence their antioxidant potential, is not a major player determining longevity.

Another role for PAs in seed longevity may be due to their structural function, binding to cell walls and providing physical protection (Pourcel *et al.*, 2007). Proanthocyanidins are structural components of the cuticle, a layer compromised in several *tt* mutants with enhanced seed permeability (Loubéry *et al.*, 2018). Following this line of reasoning, the seed longevity defects of the flavonoid mutants found by Debeaujon *et al.* (2000) may be attributed to the decrease in PAs and higher permeability of their cuticular layer. In addition, outer integument suberin also
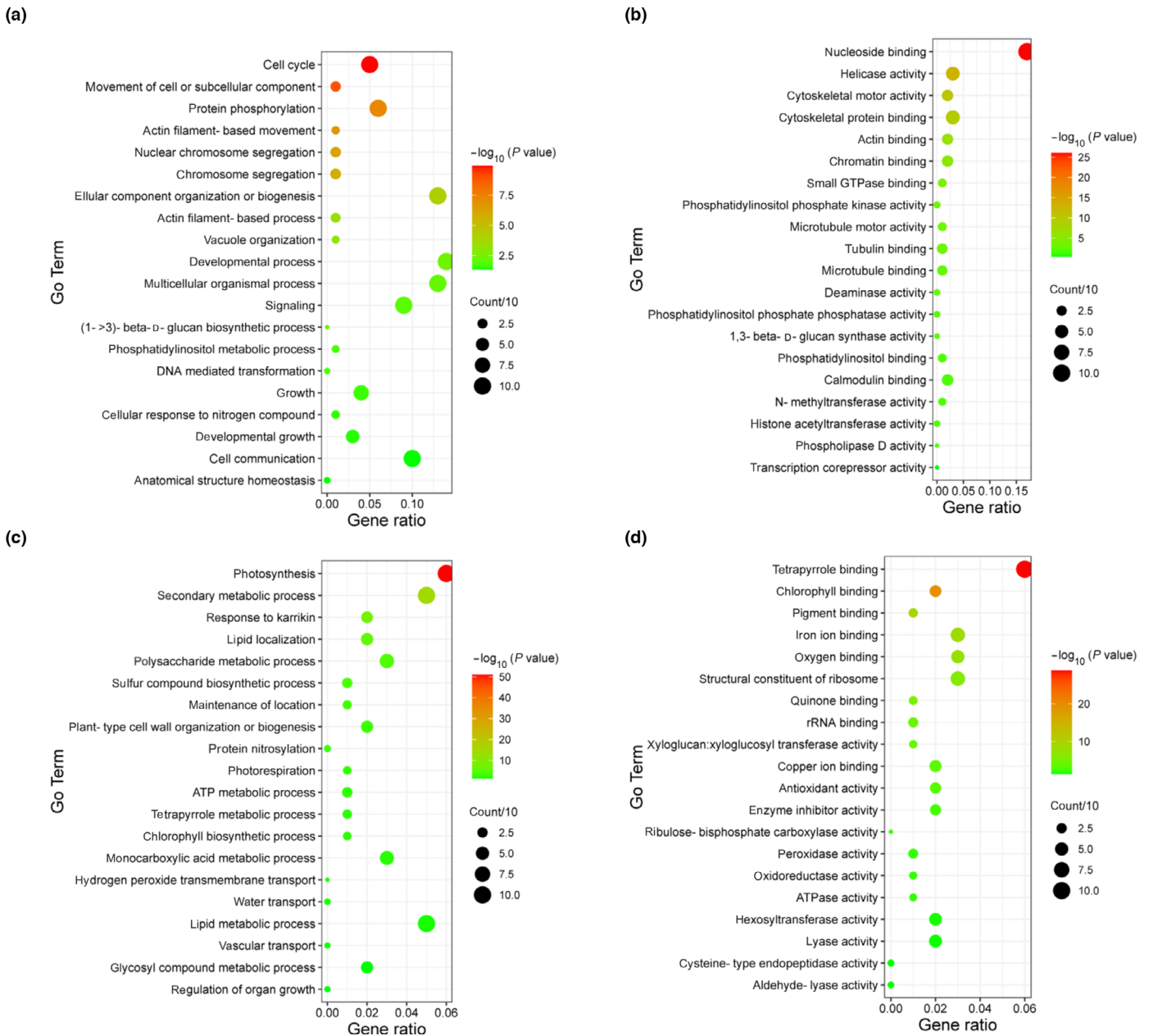
Fig. 9 Gene Ontology (GO) categories enriched on *tt7* differentially expressed genes. Top-20 nonredundant enriched GO categories in *tt7* upregulated (upper panel) and downregulated (lower panel) genes. (a, c) refer to Biological Process Terms, (b, d) refer to Molecular Function Terms. GO enrichments were obtained using AGRIGO v.2 and filtered using REVIGO (Supek *et al.*, 2011) to remove semantically redundant terms. Terms were pruned by REVIGO frequency (terms with frequency > 10% were removed) and ranked by dispensability. Full lists can be found in Supporting Information Table S4. Gene ratio: Ratio of upregulated genes in a given category divided by total number of genes in this category. Counts, number of upregulated genes in a given category. −log *P* (*P*-value in log scale after false discovery rate correction).

contributes to impermeability, and this layer is synthesized later in development, when seed longevity is being acquired (Righetti *et al.*, 2015). Suberin covers the entire seed coat, a requisite to avoid entrance of external molecules (Molina *et al.*, 2008). Mutant seeds affected in suberin synthesis have increased seed permeability and reduced longevity, and thickening this layer increases seed longevity in several species (Renard *et al.*, 2021). Among all the mutants assayed in this study, *tt7* presents the most dramatic reduction in longevity, and in contrast with others, it also shows distinctive defects in the outer integument,

including cell wall suberization and starch accumulation. *tt7* also shows the highest permeability, which would explain its extremely compromised longevity.

Interestingly, our study revealed that seeds severely defective in seed coat starch degradation also present reduced longevity, adding a new component contributing to this trait, independent of seed permeability. Digestion of starch granules in the outer integument is needed for proper cell differentiation (Andriotis *et al.*, 2010) and contributes to the structural formation of the seed surface via reinforcement of cell walls (Kim *et al.*, 2005),

which would protect the seed from external damage. These findings suggest that the most essential barriers determining seed longevity are located in the outer integument and pinpoints flavonols as regulators of its differentiation, although the contribution of the cuticle to seed permeability must also be considered (Loubéry *et al.*, 2018).

It is plausible that the reduction in longevity of other mutants defective in outer integument development, such as *apetala2* (*ap2*) (Western *et al.*, 2001), could also be caused by an altered composition of flavonols. In this regard, a recent report shows that the miR172-mediated repression of *AP2* alters flavonoid biosynthesis in apple (Ding *et al.*, 2022). Curiously, defects in lipid polyesters (suberin and cutin) have been also observed in the *transparent testa* mutant *tt15* (DeBolt *et al.*, 2009; Loubéry *et al.*, 2018). Although its flavonoid profile is altered, it does not overaccumulate kaempferol derivatives (Routaboul *et al.*, 2012), indicating that > 1 flavonoid subgroup could be interfering with suberin biosynthesis. The defects in *tt15*, however, are different from those observed in *tt7*: the inability to degrade starch is not reported for *tt15*, although its cuticle is affected (Loubéry *et al.*, 2018).

Kaempferols are key players in the regulation of many plant processes. For example, 3-O-glycosylation of kaempferol is a restriction point for the supply of the benzenoid precursor of ubiquinone (Soubeyrand *et al.*, 2018, 2021), which plays indispensable roles in plant growth and development (Liu & Lu, 2016). Similarly, catabolism of K-3,7-di-R increases during developmental senescence (Unterlander *et al.*, 2022), and it is also accumulated in response to infections by the caterpillar *Pieris brassicae* (Onkokesung *et al.*, 2014), and limits polar auxin transport and associated growth and organ development processes (Yin *et al.*, 2014; Kuhn *et al.*, 2016). The cellular levels of these compounds, however, must be tightly regulated, because accumulation of particular kaempferol derivatives over a certain threshold is detrimental and has a tremendous impact on plant development. The modified flavonol glycosylation profile in the *rol1-2* mutant, for example (with increases in K-3-R, K-3-G and another unknown kaempferol-derived compound), provokes hyponastic growth, aberrant morphology in cotyledons and defective trichome formation (Ringli *et al.*, 2008). Similarly, mutants in the *UGT78D2* gene present an altered kaempferol glycoside pattern and develop a dwarfing shoot phenotype and loss of apical dominance (Yin *et al.*, 2014), which in this case is attributed to the enhanced accumulation of K-3,7-di-R. The defects observed here for *tt7* seeds correlate with the overaccumulation of K-3-R. This compound is found in wild-type seeds, although its precise role is unknown. However, the relative expression in seed coat and embryo of the two glycosyltransferases responsible for kaempferol rhamnosylation (UGT78D1 and UGT89C1; Winter *et al.*, 2007; Belmonte *et al.*, 2013; which correlates with K-3-R and K-3-7-R being the most abundant kaempferol derivatives in seed coats and embryos, respectively; Routaboul *et al.*, 2006), suggest that K-3-R should have its main function in the seed coat. Moreover, the spatiotemporal window where *tt7* defects are visible, constrained mainly to the outer integument and starting at 9 DAP, discards early events of integument development and points more to a role in later stages of outer integument

differentiation for the cellular target of K-3-R. Similar to what occurs for K-3-7-R (Yin *et al.*, 2014), it seems that the amounts of K-3-R in the cell cannot exceed wild-type levels, which would be $< 0.1 \, \text{mg} \, \text{g}^{-1}$ (Routaboul *et al.*, 2012). Levels of K-3-R in the wild-type accession used in this study are lower than $0.1 \, \text{mg} \, \text{g}^{-1}$ (Routaboul *et al.*, 2006), and in *tt7*, these levels increase 16-fold (Fig. 7). Such an increase causes a drastic phenotype in outer integument differentiation, including defects in mucilage and suberin biosynthesis and starch degradation which affects seed longevity, uncovering processes where this compound could be involved. Within the physiological range, K-3-R levels in dry seeds are higher in natural accessions exhibiting lower longevity (Routaboul *et al.*, 2012; Renard *et al.*, 2020b), reinforcing the idea that K-3-R levels and seed longevity anticorrelate. Nevertheless, seed longevity is a highly polygenic trait (Renard *et al.*, 2020b), and detrimental factors can be compensated in some cases. The *tt4* mutant, for example, does not exhibit a dramatic reduction in longevity despite presenting high seed permeability. Similarly, the Mt-0 accession exhibits high seed longevity despite its high K-3-R levels (Routaboul *et al.*, 2012; Renard *et al.*, 2020b), discarding a strict correlation between any parameter and seed longevity. Evidence has accumulated implicating flavonols in plant growth and auxin transport modulation (Peer *et al.*, 2004; Kuhn *et al.*, 2011). Auxins are also important for the acquisition of seed longevity in the embryo (Pellizzaro *et al.*, 2018). Whether these processes are modulated by flavonoids is unknown, but the fact that *TT7* is the only flavonoid biosynthetic gene found in the co-expression network during longevity acquisition in *Medicago* and *Arabidopsis* (Righetti *et al.*, 2015) points in this direction. The altered expression of phosphatidylinositol kinases (PIPKs) and cytoskeleton-related genes in *tt7* seeds are additional evidence connecting flavonols with auxin transport in seeds, given their involvement in this process (Ischebeck *et al.*, 2013; Abu-Abie *et al.*, 2018; Ojangu *et al.*, 2018; Song *et al.*, 2021). In addition, auxin transport is repressed in *tt7* seedlings, and auxin efflux carriers PIN1 and PIN4 are delocalized (Peer *et al.*, 2004). In any case, these observations are only correlations, and whether auxins are involved in these processes or are playing a role in *tt7* seed defects will require further research.

The link between PIPK and actin in cytoskeleton dynamics is well-established (Davis *et al.*, 2007; Spiering & Hodgson, 2011; Croisé *et al.*, 2014). The transcriptomic profile of *tt7* seeds suggests dysfunction of these proteins and that the cytoskeleton could be altered in this mutant. Consequently, vesicle trafficking would be compromised, affecting seed coat cell wall synthesis and remodelling (Krishnamoorthy *et al.*, 2014), and localization of transporters or lipid transfer proteins involved in suberin formation (Deeken *et al.*, 2016), which were found to be deregulated in *tt7* seeds. The actin cytoskeleton (Chen *et al.*, 2010; Su *et al.*, 2010) and transient callose deposition (Vatén *et al.*, 2011; Wu *et al.*, 2018; Cheval *et al.*, 2020) are also mechanisms that control plasmodesmata aperture. In *tt7* seeds, the coordinated upregulation of callose synthase genes suggests that cell–cell communication could also be affected, altering sugar flux and activating starch synthesis. A complementary explanation for the *tt7* starch-excess phenotype could be the inhibition of starch-

degrading cytosolic α-glucosidases such as DPE2, given the ability of kaempferol to inhibit these enzymes (Peng *et al.*, 2016).

The readjustment of growth by alterations of the differentiation status is a strategy for plants suffering from different stresses. Given that flavonoids are involved in the response to many stressful agents, they are candidates to impact this stress-induced redistribution of growth and development (Lazar & Goodman, 2006; Jan *et al.*, 2021). Environmental conditions such as temperature and light intensity experienced by the mother plant alter the developmental programmes, leading to the acquisition of longevity and other seed traits (Nagel *et al.*, 2005; He *et al.*, 2014), and most of these cues also modify flavonoid composition (Di Ferdinando *et al.*, 2012; Macgregor *et al.*, 2015; Schulz *et al.*, 2016). Changes in flavonol composition and conjugation could be a mechanism to modulate enzymatic activities regulating cell trafficking and cell–cell communication. Interestingly, the largest variations in flavonoids found in natural accessions of Arabidopsis are in seed coat-specific flavonols, such as quercetin 3-O-rhamnoside or kaempferol derivatives (Routaboul *et al.*, 2012). The fact that the most promising QTL candidate for controlling kaempferol contents is at the genomic region where the TT7 gene is located (Routaboul *et al.*, 2012) and that TT7 is the only flavonoid biosynthetic gene of the genetic network expressed during acquisition of longevity (Righetti *et al.*, 2015) suggests that modulation of kaempferols to quercetins could be a signal to regulate this trait via cell wall reinforcements and suberin accumulation, positioning TT7 as an essential player controlling seed coat development and seed longevity.

Acknowledgements

Competing interests

None declared.

Author contributions

RN, PA, SMA and JC carried out the experiments. JG and RN conceived the original idea and wrote the manuscript. RS and EB helped in experimental design and interpretation. AH and IM performed lipid polyester measurements. AE performed flavonoid measurements.

ORCID

Eduardo Bueso (iD) https://orcid.org/0000-0002-0828-121X
Jose Gadea (iD) https://orcid.org/0000-0002-3612-7914
Isabel Molina (iD) https://orcid.org/0000-0003-3450-893X
Regina Niñoles (iD) https://orcid.org/0000-0002-7862-9509
Ramón Serrano (iD) https://orcid.org/0000-0002-4267-0016

Data availability

Data have been submitted to the GEO repository under the accession no. GSE197932.

References

Abu-Abie M, Belausov E, Hagay S, Peremyslov V, Dolja V, Sadot E. 2018. Myosin XI-K is involved in root organogenesis, polar auxin transport, and cell division. *Journal of Experimental Botany* **69**: 2869–2881.

Andriotis VM, Pike MJ, Kular B, Rawsthorne S, Smith AM. 2010. Starch turnover in developing oilseed embryos. *New Phytologist* **187**: 791–804.

Appelhagen I, Thiedig K, Nordholt N, Schmidt N, Huep G, Sagasser M, Weisshaar B. 2014. Update on transparent testa mutants from *Arabidopsis thaliana*: characterisation of new alleles from an isogenic collection. *Planta* **240**: 955–970.

Beisson F, Li Y, Bonaventure G, Pollard M, Ohlrogge JB. 2007. The acyltransferase GPAT5 is required for the synthesis of suberin in seed coat and root of Arabidopsis. *Plant Cell* **19**: 351–368.

Belmonte M, Kirkbride RC, Stone SL, Pelletier JM, Bui AQ, Yeung EC, Hashimoto M, Fei J, Harada CM, Munoz MD et al. 2013. Comprehensive developmental profiles of gene activity in regions and subregions of the Arabidopsis seed. *Proceedings of the National Academy of Sciences, USA* **110**: E434–E444.

Böhl M, Tietze S, Sokoll A, Madathil S, Pfennig F, Apostolakis J, Fahmy K, Gutzeit HO. 2007. Flavonoids affect Actin functions in cytoplasm and nucleus. *Biophysical Journal* **93**: 2767–2780.

Bowerman PA, Ramirez MV, Price MB, Helm RF, Winkel BS. 2012. Analysis of T-DNA alleles of flavonoid biosynthesis genes in Arabidopsis ecotype Columbia. *BMC Research Notes* **5**: 485.

Chen C, Zhang Y, Zhu L, Yuan M. 2010. The Actin cytoskeleton is involved in the regulation of the plasmodesmal size exclusion limit. *Plant Signalling & Behaviour* **5**: 1663–1665.

Cheval C, Samwald S, Johnston MG, de Keijzer J, Breakspear A, Liu X, Bellandi A, Kadota Y, Zipfel C, Faulkner C. 2020. Chitin perception in plasmodesmata characterizes submembrane immune-signaling specificity in plants. *Proceedings of the National Academy of Sciences, USA* **28**: 9621–9629.

Clerkx EJ, Blankestijn-De Vries H, Ruys GJ, Groot SPC, Koornneef M. 2004. Genetic differences in seed longevity of various Arabidopsis mutants. *Physiologia Plantarum* **121**: 448–461.

Croisé P, Estay-Ahumada C, Gasman S, Ory S. 2014. Rho GTPases, phosphoinositides, and Actin: a tripartite framework for efficient vesicular trafficking. *Small GTPases* **5**: e29469.

Czechowski T, Stitt M, Altmann T, Udvardi MK, Scheible WR. 2005. Genome-wide identification and testing of superior reference genes for transcript normalization in Arabidopsis. *Plant Physiology* **139**: 5–17.

Davis AJ, Im YJ, Dubin JS, Tomer KB, Boss WF. 2007. Arabidopsis phosphatidylinositol phosphate kinase 1 binds F-actin and recruits phosphatidylinositol 4-kinase β1 to the Actin cytoskeleton. *Journal of Biological Chemistry* **11**: 14121–14131.

De Giorgi J, Piskurewicz U, Loubéry S, Utz-Pugin A, Bailly C, Mène-Saffrané L, Lopez-Molina L. 2015. An endosperm-associated cuticle is required for arabidopsis seed viability, dormancy and early control of germination. *PLoS Genetics* **17**: e1005708.

De Silva NDG, Boutin C, Lukina AO, Western TL, Molina I, Rowland O. 2021. Seed coat suberin forms a barrier against chromium (Cr^{3+}) during early seed germination in *Arabidopsis thaliana. Environmental and Experimental Botany* **191**: 104632.

Debeaujon I, Léon-Kloosterziel KM, Koornneef M. 2000. Influence of the testa on seed dormancy, germination, and longevity in Arabidopsis. *Plant Physiology* **122**: 403–414.

DeBolt S, Scheible WR, Schrick K, Auer M, Beisson F, Bischoff V, Bouvier-Navé P, Carroll A, Hematy K, Li Y et al. 2009. Mutations in UDP-Glucose: sterol glucosyltransferase in Arabidopsis cause transparent testa phenotype and suberization defect in seeds. *Plant Physiology* **151**: 78–87.

Deeken R, Saupe S, Klinkenberg J, Riedel M, Leide J, Hedrich R, Mueller TD. 2016. The nonspecific lipid transfer protein AtLtpI-4 is involved in suberin formation of *Arabidopsis thaliana* crown galls. *Plant Physiology* **172**: 1911–1927.

Di Ferdinando M, Brunetti C, Fini A, Tattini M. 2012. Flavonoids as antioxidants in plants under abiotic stresses. In: Prasad MNV, Ahmad P, eds. *Abiotic stress responses in plants: metabolism, productivity and sustainability.* New York, NY, USA: Springer, 159–179.

Ding T, Tomes S, Gleave AP, Zhang H, Dare AP, Plunkett B, Espley RV, Luo Z, Zhang R, Allan AC et al. 2022. microRNA172 targets APETALA2 to regulate flavonoid biosynthesis in apple (*Malus domestica*). *Horticultural Research* **18**: uhab007.

Groot SP, Surki AA, de Vos RC, Kodde J. 2012. Seed storage at elevated partial pressure of oxygen, a fast method for analysing seed ageing under dry conditions. *Annals of Botany* **110**: 1149–1159.

Grunewald W, De Smet I, De Rybel B, Robert HS, van de Cotte B, Willemsen V, Gheysen G, Weijers D, Friml J, Beeckman T. 2013. Tightly controlled WRKY23 expression mediates Arabidopsis embryo development. *EMBO Reports* **14**: 1136–1142.

Haughn G, Chaudhury A. 2005. Genetic analysis of seed coat development in Arabidopsis. *Trends in Plant Science* **10**: 472–477.

He H, de Souza VD, Snoek LB, Schnabel S, Nijveen H, Hilhorst H, Bentsink L. 2014. Interaction between parental environment and genotype affects plant and seed performance in Arabidopsis. *Journal of Experimental Botany* **65**: 6603–6615.

Hernández I, Alegre L, Van Breusegem F, Munné-Bosch S. 2009. How relevant are flavonoids as antioxidants in plants? *Trends in Plant Science* **14**: 125–132.

Hildreth SB, Littleton ES, Clark LC, Puller GC, Kojima S, Winkel BSJ. 2022. Mutations that alter Arabidopsis flavonoid metabolism affect the circadian clock. *The Plant Journal* **110**: 932–945.

Ischebeck T, Werner S, Krishnamoorth P, Lerche J, Meijón M, Stenzel I, Löfke C, Wiessner T, Im YJ, Perera IY et al. 2013. Phosphatidylinositol 4,5-bisphosphate influences PIN polarization by controlling clathrin-mediated membrane trafficking in Arabidopsis. *Plant Cell* **25**: 4894–4911.

Jan R, Kim N, Lee SH, Khan MA, Asaf S, Lubna PJR, Asif S, Lee IJ, Kim KM. 2021. Enhanced flavonoid accumulation reduces combined salt and heat stress through regulation of transcriptional and hormonal mechanisms. *Frontiers in Plant Science* **21**: 796956.

Jones P, Messner B, Nakajima J, Schäffner AR, Saito K. 2003. UGT73C6 and UGT78D1, glycosyltransferases involved in flavonol glycoside biosynthesis in *Arabidopsis thaliana. Journal of Biological Chemistry* **278**: 43910–43918.

Kerhoas L, Aouak D, Cingöz A, Routaboul JM, Lepiniec L, Einhorn J, Birlirakis N. 2006. Structural characterization of the major flavonoid glycosides from *Arabidopsis thaliana* seeds. *Journal of Agricultural and Food Chemistry* **6**: 6603–6612.

Kim YC, Nakajima M, Nakayama A, Yamaguchi I. 2005. Contribution of gibberellins to the formation of Arabidopsis seed coat through starch degradation. *Plant & Cell Physiology* **46**: 1317–1325.

Kong D, Zhan Y, Yamori T, Duan H, Jin M. 2011. Inhibitory activity of flavonoids against class I phosphatidylinositol 3-kinase isoforms. *Molecules* **16**: 5159–5167.

Kötting O, Santelia D, Edner C, Eicke S, Marthaler T, Gentry MS, Comparot-Moss S, Chen J, Smith AM, Steup M et al. 2009. STARCH-EXCESS4 is a laforin-like phosphoglucan phosphatase required for starch degradation in *Arabidopsis thaliana. Plant Cell* **21**: 334–346.

Krishnamoorthy P, Sanchez-Rodriguez C, Heilman I, Persson S. 2014. Regulatory roles of phosphoinositides in membrane trafficking and their potential impact on cell-wall synthesis and re-modelling. *Annals of Botany* **114**: 1049–1057.

Kuhn BM, Errafi S, Bucher R, Dobrev P, Geisler M, Bigler L, Zažímalová E, Ringli C. 2016. 7-Rhamnosylated flavonols modulate homeostasis of the plant hormone auxin and affect plant development. *Journal of Biological Chemistry* **291**: 5385–5395.

Kuhn BM, Geisler M, Bigler L, Ringli C. 2011. Flavonols accumulate asymmetrically and affect auxin transport in Arabidopsis. *Plant Physiology* **156**: 585–595.

Lazar G, Goodman HM. 2006. MAX1, a regulator of the flavonoid pathway, controls vegetative axillary bud outgrowth in Arabidopsis. *Proceedings of the National Academy of Sciences, USA* **10**: 472–476.

Lee KM, Lee DE, Seo SK, Hwang MK, Heo YS, Lee KW, Lee HJ. 2010. Phosphatidylinositol 3-kinase, a novel target molecule for the inhibitory effects of kaempferol on neoplastic cell transformation. *Carcinogenesis* **31**: 1338–1343.

Lepiniec L, Debeaujon I, Routaboul JM, Baudry A, Pourcel L, Nesi N, Caboche M. 2006. Genetics and biochemistry of seed flavonoids. *Annual Review of Plant Biology* **57**: 405–430.

Liu M, Lu S. 2016. Plastoquinone and ubiquinone in plants: biosynthesis, physiological function and metabolic engineering. *Frontiers in Plant Science* **16**: 1898.

Loubéry S, De Giorgi J, Utz-Pugin A, Demonsais L, Lopez-Molina L. 2018. A maternally deposited endosperm cuticle contributes to the physiological defects of transparent testa seeds. *Plant Physiology* **177**: 1218–1233.

Lu Y, Savage LJ, Ajjawi I, Imre KM, Yoder DW, Benning C, Dellapenna D, Ohlrogge JB, Osteryoung KW, Weber AP et al. 2008. New connections across pathways and cellular processes: industrialized mutant screening reveals novel associations between diverse phenotypes in Arabidopsis. *Plant Physiology* **146**: 1482–1500.

MacGregor DR, Kendall SL, Florance H, Fedi F, Moore K, Paszkiewicz K, Smirnoff N, Penfield S. 2015. Seed production temperature regulation of primary dormancy occurs through control of seed coat phenylpropanoid metabolism. *New Phytologist* **205**: 642–652.

Molina I, Ohlrogge JB, Pollard M. 2008. Deposition and localization of lipid polyester in developing seeds of Brassica napus and *Arabidopsis thaliana. The Plant Journal* **53**: 437–449.

Nagel M, Kranner I, Neumann K, Rolletschek H, Seal CE, Colville L, Fernández-Marín B, Börner A. 2005. Genome-wide association mapping and biochemical markers reveal that seed ageing and longevity are intricately affected by genetic background and developmental and environmental conditions in barley. *Plant, Cell & Environment* **38**: 1011–1022.

Ojangu EL, Ilau B, Tanner K, Talts K, Ihoma E, Dolja VV, Paves H, Truve E. 2018. Class XI myosins contribute to auxin response and senescence-induced cell death in Arabidopsis. *Frontiers in Plant Science* **27**: 1570.

Oñate-Sánchez L, Vicente-Carbajosa J. 2008. DNA-free RNA isolation protocols for *Arabidopsis thaliana*, including seeds and siliques. *BMC Research Notes* **20**: 93.

Onkokesung N, Reichelt M, van Doorn A, Schuurink RC, van Loon JJ, Dicke M. 2014. Modulation of flavonoid metabolites in *Arabidopsis thaliana* through overexpression of the MYB75 transcription factor: role of kaempferol-3,7-dirhamnoside in resistance to the specialist insect herbivore *Pieris brassicae. Journal of Experimental Botany* **65**: 2203–2217.

Owens DK, Alerding AB, Crosby KC, Bandara AB, Westwood JH, Winkel BS. 2008. Functional analysis of a predicted flavonol synthase gene family in Arabidopsis. *Plant Physiology* **147**: 1046–1061.

Peer WA, Bandyopadhyay A, Blakeslee JJ, Makam SN, Chen RJ, Masson PH, Murphy AS. 2004. Variation in expression and protein localization of the PIN family of auxin efflux facilitator proteins in flavonoid mutants with altered auxin transport in *Arabidopsis thaliana. Plant Cell* **16**: 1898–1911.

Peer WA, Murphy AS. 2007. Flavonoids and auxin transport: modulators or regulators? *Trends in Plant Science* **12**: 556–563.

Pellizzaro A, Neveu M, Lalanne D, Ly VB, Kanno Y, Seo M, Leprince O, Buitink J. 2018. A role for auxin signaling in the acquisition of longevity during seed maturation. *New Phytologist* **225**: 284–296.

Peng X, Zhang G, Liao Y, Gong D. 2016. Inhibitory kinetics and mechanism of kaempferol on α-glucosidase. *Food Chemistry* 1: 207–215.

Pourcel L, Routaboul JM, Cheynier V, Lepiniec L, Debeaujon I. 2007. Flavonoid oxidation in plants: from biochemical properties to physiological functions. *Trends in Plant Science* 12: 29–36.

Pourcel L, Routaboul JM, Kerhoas L, Caboche M, Lepiniec L, Debeaujon I. 2005. TRANSPARENT TESTA10 encodes a laccase-like enzyme involved in oxidative polymerization of flavonoids in Arabidopsis seed coat. *Plant Cell* 17: 2966–2980.

Renard J, Martínez-Almonacid I, Queralta-Castillo I, Sonntag A, Hashim A, Bissoli G, Campos L, Muñoz-Bertomeu J, Niñoles R, Roach T et al. 2021. Apoplastic lipid barriers regulated by conserved homeobox transcription factors extend seed longevity in multiple plant species. *New Phytologist* 231: 679–694.

Renard J, Martínez-Almonacid I, Sonntag A, Molina I, Moya-Cuevas J, Bissoli G, Muñoz-Bertomeu J, Faus I, Niñoles R, Shigeto J et al. 2020a. PRX2 and PRX25, peroxidases regulated by COG1, are involved in seed longevity in Arabidopsis. *Plant, Cell & Environment* 43: 315–326.

Renard J, Niñoles R, Martínez-Almonacid I, Gayubas B, Mateos-Fernández R, Bissoli G, Bueso E, Serrano R, Gadea J. 2020b. Identification of novel seed longevity genes related to oxidative stress and seed coat by genome-wide association studies and reverse genetics. *Plant, Cell & Environment* 43: 2523–2539.

Righetti K, Vu JL, Pelletier S, Vu BL, Glaab E, Lalanne D, Pasha A, Patel RV, Provart NJ, Verdier J et al. 2015. Inference of longevity-related genes from a robust coexpression network of seed maturation identifies regulators linking seed storability to biotic defense-related pathways. *Plant Cell* 27: 2692–2708.

Ringli C, Bigle L, Kuhn BM, Leiber RM, Diet A, Santelia D, Frey B, Pollmann S, Klein M. 2008. The modified flavonol glycosylation profile in the Arabidopsis rol1 mutants results in alterations in plant growth and cell shape formation. *Plant Cell* 20: 1470–1481.

Routaboul JM, Dubos C, Beck G, Marquis C, Bidzinski P, Loudet O, Lepiniec L. 2012. Metabolite profiling and quantitative genetics of natural variation for flavonoids in Arabidopsis. *Journal of Experimental Botany* 63: 3749–3764.

Routaboul JM, Kerhoas L, Debeaujon I, Pourcel L, Caboche M, Einhorn J, Lepiniec L. 2006. Flavonoid diversity and biosynthesis in seed of *Arabidopsis thaliana*. *Planta* 224: 96–107.

Schulz E, Tohge T, Zuther E, Fernie AR, Hincha DK. 2016. Flavonoids are determinants of freezing tolerance and cold acclimation in *Arabidopsis thaliana*. *Science Reports* 23: 34027.

Shirley BW, Kubasek WL, Storz G, Bruggemann E, Koornneef M, Ausubel FM, Goodman HM. 1995. Analysis of Arabidopsis mutants deficient in flavonoid biosynthesis. *The Plant Journal* 8: 659–671.

Song L, Wang Y, Guo Z, Lam SM, Shui G, Cheng Y. 2021. NCP2/RHD4/ SAC7, SAC6 and SAC8 phosphoinositide phosphatases are required for PtdIns4P and PtdIns(4,5)P2 homeostasis and Arabidopsis development. *New Phytologist* 231: 713–725.

Soubeyrand E, Johnson TS, Latimer S, Block A, Kim J, Colquhoun TA, Butelli E, Martin C, Wilson MA, Basset GJ. 2018. The peroxidative cleavage of kaempferol contributes to the biosynthesis of the benzenoid moiety of ubiquinone in plants. *Plant Cell* 30: 2910–2921.

Soubeyrand E, Latimer S, Bernert AC, Keene SA, Johnson TS, Shin D, Block AK, Colquhoun TA, Schäffner AR, Kim J et al. 2021. 3-O-glycosylation of kaempferol restricts the supply of the benzenoid precursor of ubiquinone (Coenzyme Q) in *Arabidopsis thaliana*. *Phytochemistry* 186: 112738.

Spiering D, Hodgson L. 2011. Dynamics of the rho-family small GTPases in actin regulation and motility. *Cell Adhesion & Migration* 5: 170–180.

Streb S, Eicke S, Zeeman SC. 2012. The simultaneous abolition of three starch hydrolases blocks transient starch breakdown in Arabidopsis. *Journal of Biological Chemistry* 7: 41745–41756.

Su S, Liu Z, Chen C, Zhang Y, Wang X, Zhu L, Miao L, Wang XC, Yuan M. 2010. Cucumber mosaic virus movement protein severs actin filaments to increase the plasmodesmal size exclusion limit in tobacco. *Plant Cell* 22: 1373–1387.

Supek F, Bošnjak M, Škunca N, Šmuc T. 2011. REVIGO summarizes and visualizes long lists of gene ontology terms. *PLoS ONE* 6: e21800.

Unterlander N, Mats L, McGary LC, Gordon HOW, Bozzo GG. 2022. Kaempferol rhamnoside catabolism in rosette leaves of senescing Arabidopsis and postharvest stored radish. *Planta* 11: 36.

Vatén A, Dettmer J, Wu S, Stierhof YD, Miyashima S, Yadav SR, Roberts CJ, Campilho A, Bulone V, Lichtenberger R et al. 2011. Callose biosynthesis

regulates symplastic trafficking during root development. *Developmental Cell* 13: 1144–1155.

Waese J, Fan J, Pasha A, Yu H, Fucile G, Shi R, Cumming M, Kelley LA, Sternberg MJ, Krishnakumar V et al. 2017. ePlant: visualizing and exploring multiple levels of data for hypothesis generation in plant biology. *Plant Cell* 29: 1806–1821.

Wang ZP, Xing HL, Dong L, Zhang HY, Han CY, Wang XC, Chen QJ. 2015. Egg cell-specific promoter-controlled CRISPR/Cas9 efficiently generates homozygous mutants for multiple target genes in Arabidopsis in a single generation. *Genome Biology* 21: 144.

Western TL, Burn J, Tan WL, Skinner DJ, Martin-McCaffrey L, Moffatt BA, Haughn GW. 2001. Isolation and characterization of mutants defective in seed coat mucilage secretory cell development in Arabidopsis. *Plant Physiology* 127: 998–1011.

Windsor JB, Symonds VV, Mendenhall J, Lloyd AM. 2000. Arabidopsis seed coat development: morphological differentiation of the outer integument. *The Plant Journal* 22: 483–493.

Winter D, Vinegar B, Nahal H, Ammar R, Wilson GV, Provart NJ. 2007. An "electronic fluorescent pictograph" browser for exploring and analyzing large-scale biological data sets. *PLoS ONE* 8: e718.

Wu SW, Kumar R, Iswanto ABB, Kim JY. 2018. Callose balancing at plasmodesmata. *Journal of Experimental Botany* 26: 5325–5339.

Yin R, Han K, Heller W, Albert A, Dobrev PI, Zažímalová E, Schäffner AR. 2014. Kaempferol 3-O-rhamnoside-7-O-rhamnoside is an endogenous flavonol inhibitor of polar auxin transport in Arabidopsis shoots. *New Phytologist* 201: 466–475.

Yonekura-Sakakibara K, Nakabayashi R, Sugawara S, Tohge T, Ito T, Koyanagi M, Kitajima M, Takayama H, Saito K. 2014. A flavonoid 3-O-glucoside: 2′′-O-glucosyltransferase responsible for terminal modification of pollen-specific flavonols in *Arabidopsis thaliana*. *The Plant Journal* 79: 769–782.

Yonekura-Sakakibara K, Tohge T, Niida R, Saito K. 2007. Identification of a flavonol 7-O-rhamnosyltransferase gene determining flavonoid pattern in Arabidopsis by transcriptome coexpression analysis and reverse genetics. *Journal of Biological Chemistry* 18: 14932–14941.

Yu TS, Kofler H, Häusler RE, Hille D, Flügge UI, Zeeman SC, Smith AM, Kossmann J, Lloyd J, Ritte G et al. 2001. The Arabidopsis sex1 mutant is defective in the R1 protein, a general regulator of starch degradation in plants, and not in the chloroplast hexose transporter. *Plant Cell* 13: 1907–1918.

Zhu J, Bailly A, Zwiewka M, Sovero V, Di Donato M, Ge P, Oehri J, Aryal B, Hao P, Linnert M et al. 2016. Twisted DWARF1 mediates the action of auxin transport inhibitors on actin cytoskeleton dynamics. *Plant Cell* 28: 930–948.

Zou M, Ren H, Li J. 2019. An auxin transport inhibitor targets villin-mediated actin dynamics to regulate polar auxin transport. *Plant Physiology* 181: 161–178.

Supporting Information

Additional Supporting Information may be found online in the Supporting Information section at the end of the article.

Fig. S1 Flavonoid content of wild-type and *tt7* seeds.

Fig. S2 Spatial distribution of flavonols in embryos (a) and seed coat (b) of WS and *tt7-4* seeds (7 DAP) using diphenylboric acid 2-aminoethyl ester staining.

Fig. S3 *tt7* embryos are viable and develop normally.

Fig. S4 *tt* mutant embryos are viable and can reduce tetrazolium salts.

Fig. S5 Mucilage biosynthesis is impaired in *tt7-4*.

Fig. S6 Mucilage and seed coat lipid polyesters analysis of the *tt7-7* mutant.

Fig. S7 Transmission electron microscopy images of WS and *tt7-4* seed coats.

Fig. S8 *tt7* integuments at 3 d after pollination.

Fig. S9 Transmission electron microscopy images of WS (a) and *tt7-4* (b) seed coats at 9 d after pollination.

Fig. S10 *tt7-7* seeds accumulate starch.

Fig. S11 Starch accumulation in *tt7-4* leaves.

Fig. S12 Seed coat starch accumulation in different *tt* mutants.

Fig. S13 Sequence alignment of amplicons genotyped for WS, *tt3-4 tt7cr* and *fls1-7 tt7cr* homozygous mutants.

Fig. S14 Transmission electron microscopy analysis of seed coats of *fls1-3 7 tt7cr* (L38 and L47) and *tt3-4 tt7cr* (L20 and L8) mutants.

Fig. S15 Flavonoid content in *tt3-4 tt7cr* seeds.

Fig. S16 Sequence alignment of amplicons genotyped for WS, *ugt78d1 tt7cr* and *ugt89c1 tt7cr* homozygous mutants.

Fig. S17 Sudan Red7 staining on Col-0, *tt7-7* and *ugt78d1 tt7cr* showing polyester layers.

Fig. S18 Expression pattern of *UGT73C6*, *UGT78D1* and *UGT89C1* in developing seeds.

Fig. S19 Seed coat starch accumulation and seed permeability of starch-accumulating mutants.

Fig. S20 Venn diagram showing intersection of differentially expressed genes obtained in this study for *tt7-7* seeds vs those obtained by Hildreth *et al.* (2022) for *tt4* in seedlings.

Methods S1 Supplemental methods.

Table S1 Mutants used in this study.

Table S2 Primers used in this study.

Table S3 Differentially expressed genes between 8 d after pollination wild-type and *tt7-7* seeds.

Table S4 Gene Ontology categories enriched on differentially expressed genes between wild-type and *tt7* 8 d after pollination seeds.

Please note: Wiley is not responsible for the content or functionality of any Supporting Information supplied by the authors. Any queries (other than missing material) should be directed to the *New Phytologist* Central Office.